Introduction to Solar Physics

Sami K. Solanki

IMPRS lectures
January 2005

Structure of lectures I

- Introduction and overview
- Core and interior: energy generation and standard solar model
- Solar radiation and spectrum
  - Solar spectrum
  - Radiative transfer
  - Formation of absorption and emission lines
- Convection: The convection zone and granulation etc.
- Solar oscillations and helioseismology
- Solar rotation

Structure of lectures II

- The solar atmosphere: structure
  - Photosphere
  - Chromosphere
  - Transition Region
  - Corona
  - Solar wind and heliosphere
- The magnetic field
  - Zeeman effect and Unno-Rachkovsky equations
  - Magnetic elements and sunspots
  - Chromospheric and coronal magnetic field
  - The solar cycle
  - Coronal heating
  - MHD equations & dynamo: see lectures by Ferriz Mas

Structure of lectures III: next time

- Explosive and eruptive phenomena
  - Flares
  - CMEs
  - Explosive events
- Sun-Earth connection
  - CMEs and space weather
  - Longer term variability and climate
- Solar-stellar connection
  - Activity-rotation relationship
  - Sunspots vs. starspots

The Sun: a brief overview

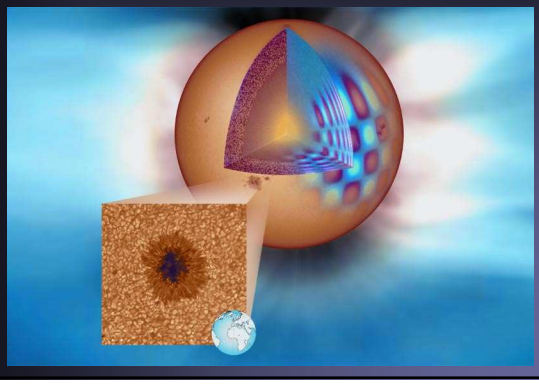

The Sun, our star

- The Sun is a normal star: middle aged (4.5 Gyr) main sequence star of spectral type G2
- The Sun is a special star: it is the only star on which we can resolve the spatial scales on which fundamental processes take place.
- The Sun is a special star: it provides almost all the energy to the Earth
- The Sun is a special star: it provides us with a unique laboratory in which to learn about various branches of physics.

The Sun: Overview

The Sun: a few numbers

- Mass = 1.99 10^{30} kg (= 1 $M_\odot$)
- Average density = 1.4 g/cm^3
- Luminosity = 3.84 10^{26} W (= 1 $L_\odot$)
- Effective temperature = 5777 K (G2 V)
- Core temperature = 15 10^6 K
- Surface gravitational acceleration g = 274 m/s^2
- Age = 4.55 10^9 years (from meteorite isotopes)
- Radius = 6.96 10^5 km
- Distance = 1 AU = 1.496 (+/-0.025) 10^8 km
- 1 arc sec = 722±12 km on solar surface (elliptical Earth orbit)
- Rotation period = 27 days at equator (sidereal, i.e. as seen from Earth; Carrington rotation)

The Sun's Structure

Solar interior:

- Everything below the Sun's (optical) surface
- Divided into hydrogen-burning core, radiative and convective zones

Solar atmosphere:

- Directly observable part of the Sun.
- Divided into photosphere, chromosphere, corona, heliosphere

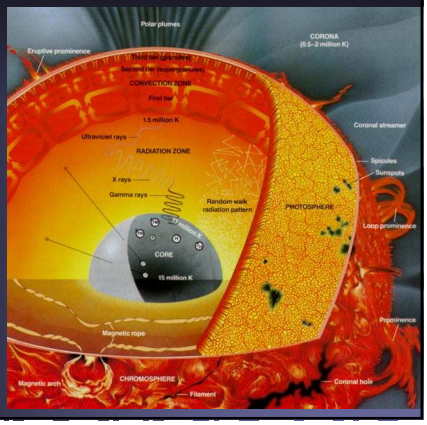

The solar surface

- Since solar material does not exhibit a phase transition (e.g. from solid or liquid to gaseous as for the Earth), a standard way to define the solar surface is through its radiation.
- The photons travelling from the core outwards make a random walk, since they are repeatedly absorbed and reemitted. The mean free path increases rapidly with radial distance from the solar core (as the density and opacity decrease).
- A point is reached where the average mean free path becomes so large that the photons escape from the Sun. This point is defined as the solar surface. It corresponds to optical depth $\tau = 1$. Its height depends on λ.
- Often $\tau = 1$ at λ=5000 Å is used as a standard for the solar surface.

Wide range of physical parameters

- The Sun presents a wide variety of physical phenomena and processes, between solar core and corona.
- E.g. Gas density varies by ≈ 30 orders of magnitude, temperature by 4 orders, relevant time scales from 10^{-10} sec to 10 Gyr

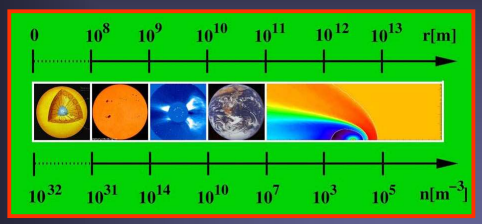

➔Different observational and theoretical techniques needed to study different parts of Sun, e.g. helioseismology & nuclear physics for interior, polarimetry & MHD for magnetism, etc.

Solar physics in relation to other branches of physics

Solar Physics in Relation to Other Fields

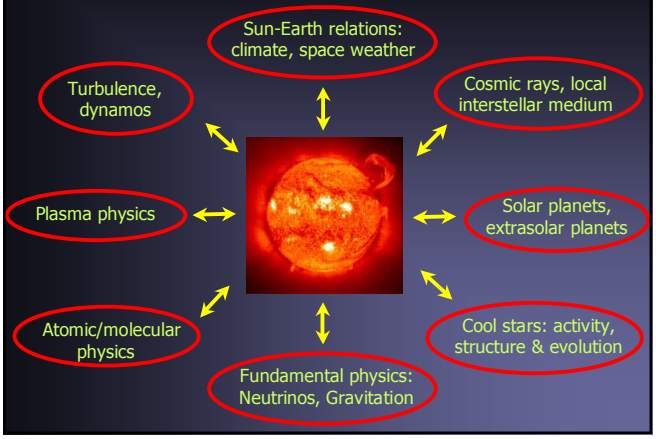

The Sun as a plasma physics lab.

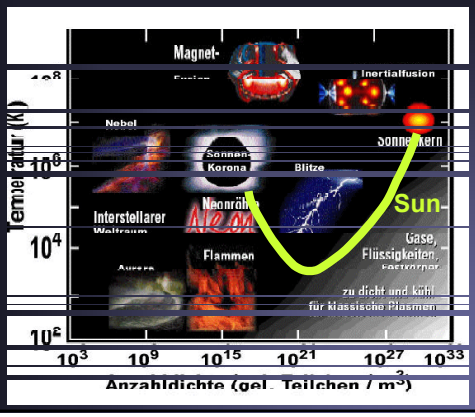

Solar Tests of Gravitational Physics

- Curved light path in solar gravitational field ➔ Test of General Relativity
- Red shift of solar spectral lines ➔ Test of EEP
- Oblate shape of Sun ➔ Quadrupol moment of solar gravitational field: Test of Brans-Dicke theory (R. Mecheri)
- Comparison of solar evolution models with observations ➔ Limits on evolution of fundamental constants
- Polarization of solar spectral lines: Tests gravitational birefringence ➔ Tests of equivalence principle & alternative theories of gravity (O. Preuss)

The Sun and particle physics

- The fact that the rate of neutrinos measured by the Homestake ^{37}Cl detector is only 1/3 of that predicted by standard solar models was for > 30 years one of the major unsolved problems of physics.
- Possible resolutions:
  - Standard solar model is wrong
  - Neutrino physics is incomplete
- Recent findings from SNO and Superkamiokande: Problem lies with the neutrino physics

➔ Standard model of particle physics needs to be revised

- Nobel prize 2002 for R. Davies for discovery of the solar neutrino problem.

Solar physics and astrophysics

- Phenomena happening all over the universe can be best studied at close distances, where the relevant physical processes can be spatially resolved (same for solar planets).
- E.g. magnetic activity, is present on innumerable stars, in accretion disks, in jets, in the interstellar medium, etc., but the relevant spatial scales can generally not be resolved. The Sun provides a key.
- Radio astronomy, radiative transfer, spectropolarimetry, asteroseismolgy, etc. are techniques first developed to study the Sun

Which stars have magnetic fields or show magnetic activity?

- Best studied star: Sun
- F, G, K & M stars (outer convection zones) show magnetic activity & have <B> fields of G-kG.
- Early type stars: Ap, Bp, (kG-100kG), Be (100G)
- White dwarfs have B ≈ kG-10^9 G, no activity
- Not on diagram: pulsars

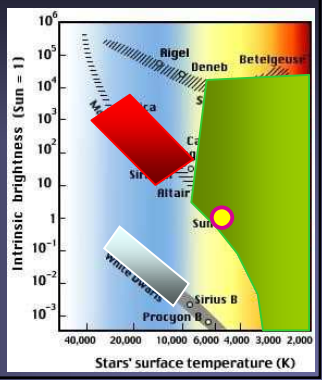

The Sun compared with active stars

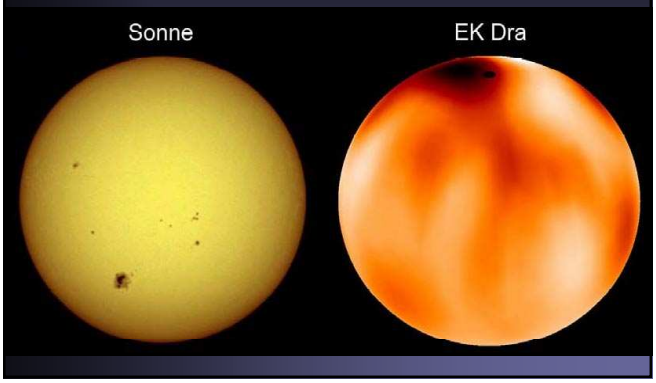

Sun, Earth and planets

- Solar output affects the magnetospheres and atmospheres of planets
- Solar energy is responsible for providing a habitable environment on Earth
- Solar evolution and liquid water on Mars...

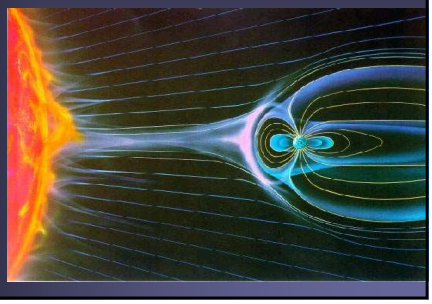

The solar interior

The Sun's core

- In the Sun's core mass is turned into energy.
- Nuclear reactions burn 7×10^{11} kg/s of hydrogen into helium.
- Inside the core the particle density and temperature are so high, that individual protons ram into each other at sufficient speed to overcome the Coulomb barrier, forming heavier He atoms and releasing energy

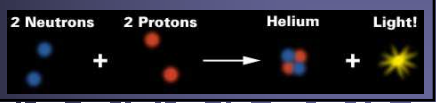

Nuclear reactions in cores of stars

- Sun gains practically all its energy from the reaction $4p \rightarrow \alpha + 2e^{+} + 2\nu = {}^{4}He + 2e^{+} + 2\nu$
- Two basic routes
  - p-p chain: yields about 99% of energy in Sun
  - CNO cycle : 1% of energy released in present day Sun (but dominant form of energy release in hotter stars)
- Both chains yield a total energy Q of 26.7 MeV, mainly in the form of γ-radiation Q_γ (which is absorbed and heats the gas) and neutrinos Q_ν (which escapes from the Sun).

Nuclear reactions of pp-chain

- p=proton
- d=deuterium
- α=Helium
- γ=radiation
- ν=neutrino
- 2nd reaction replaces step 3 of 1st reaction

Table 2.1. Nuclear reactions of the pp chains. Energy values according to Bahcall and Ulrich (1988) and Caughlan and Fowler (1988)

	Reaction	Q'[MeV]	Q_ν[MeV]	Rate symbol
ppI	$p(p,e^+\nu)d$	1.177	0.265	λ_{pp}
	$d(p,\gamma)^3He$	5.494		λ_{pd}
	$^3He(^3He,2p)\alpha$	12.860		λ_{33}
ppII	$^3He(\alpha,\gamma)^7Be$	1.586		λ_{34}
	$^7Be(e^-,\nu\gamma)^7Li$	0.049	0.815	λ_{e7}
	$^7Li(p,\alpha)\alpha$	17.346		λ'_{17}
ppIII	$^7Be(p,\gamma)^8B$	0.137		λ_{17}
	$^8B(,e^+\nu)^8Be^*$	8.367	6.711	λ_8
	$^8Be^*(,\alpha)\alpha$	2.995		λ'_8

- 3rd reaction replaces steps 2+3 of 2nd reaction
- Branching ratios:
  - 1st vs. 2nd + 3rd 87 : 13
  - 2nd vs. 3rd → 13 : 0.015

Nuclear reactions of CNO-cycle

- C, N and O act only as catalysts: Basically the same things happens as with proton chain.

Table 2.2. Nuclear reactions of the CNO cycle. Energy values according to Bahcall and Ulrich (1988) and Caughlan and Fowler (1988)

Reaction	Q'[MeV]	Q_ν[MeV]	Rate symbol
$^{12}C(p,\gamma)^{13}N$	1.944		λ_{p12}
$^{13}N(,e^+\nu)^{13}C$	1.513	0.707	λ_{13}
$^{13}C(p,\gamma)^{14}N$	7.551		λ_{p13}
$^{14}N(p,\gamma)^{15}O$	7.297		λ_{p14}
$^{15}O(,e^+\nu)^{15}N$	1.757	0.997	λ_{15}
$^{15}N(p,\alpha)^{12}C$	4.966		λ_{p15}

Temperature dependence of pp-chain and CNO cycle

- p-p chain in cool main-sequence stars
- CNO cycle in hot main-sequence stars
- Triple alpha process in red giants: 3He → C

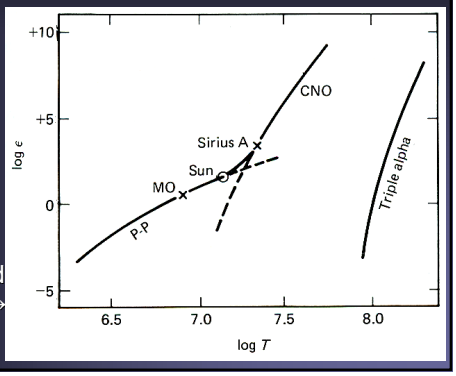

Solar neutrinos

- Neutrinos, ν, are produced at various stages of the pp-chain.
- Neutrinos are also produced by the reaction: p(p e^- , ν)d , so-called pep reaction. Being a 3-body reaction it is too rare to contribute to the energy, but does contribute to the number of ν.

	Reaction	Q'[MeV]	Q_ν[MeV]
ppI	$p(p,e^+\nu)d$	1.177	0.265
	$d(p,\gamma)^3He$	5.494	
	$^3He(^3He,2p)\alpha$	12.860	
ppII	$^3He(\alpha,\gamma)^7Be$	1.586	
	$^7Be(e^-,\nu\gamma)^7Li$	0.049	0.815
	$^7Li(p,\alpha)\alpha$	17.346	
ppIII	$^7Be(p,\gamma)^8B$	0.137	
	$^8B(,e^+\nu)^8Be^*$	8.367	6.711
	$^8Be^*(,\alpha)\alpha$	2.995	

Solar neutrino spectrum

- Continua: number/(cm^2 s MeV)
- Lines: number/(cm^2 s)
- Bars at top & shading: sensitivity of different materials to ν

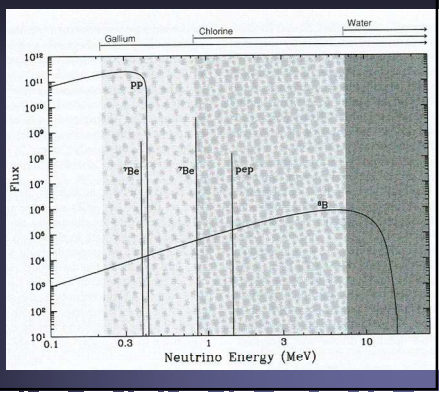

Solar neutrinos II

- Since 1968 the Homestake ^{37}Cl experiment has given a value of 2.1 ± 0.3 snu (1snu =1 ν / 10^{36} target atoms)
- Standard solar models predict: 7±2 snu

➔Solar Neutrino Problem!

- In 1980s & 90s water based Kamiokande and larger Superkamiokande detectors found that approximately half the rare, high energy ^{8}B ν were missing.
- ^{71}Ga experiments (GALLEX at Gran Sasso and SAGE in Russia) showed that the neutrino flux was too low, even including the p(p,e$^+$ ν)d neutrinos.

Results of various neutrino experiments

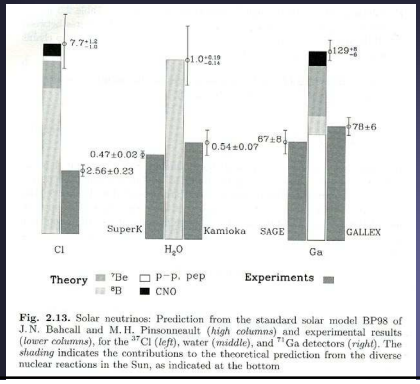

Fig. 2.13. Solar neutrinos: Prediction from the standard solar model BP98 of J.N. Bahcall and M.H. Pinsonneault (*high columns*) and experimental results (*lower columns*), for the ^{37}Cl (*left*), water (*middle*), and ^{71}Ga detectors (*right*). The *shading* indicates the contributions to the theoretical prediction from the diverse nuclear reactions in the Sun, as indicated at the bottom

Solar neutrinos III

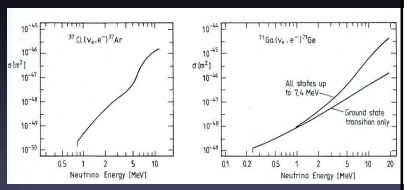

- Sensitivity of H_2O, ^{71}Ga and ^{37}Cl to ν increases ~ exponentially with increasing energy.

➔ Homestake ^{37}Cl detector and (Super-) Kamiokande see mainly high-energy ν from rare β^+-decay of ^8B.

- Branching ratios between the various chains: central for predicting exact ν-flux detectable by ^{37}Cl & H_2O
- Branching ratios depend very sensitively on T(r=0), while total ν-flux depends only linearly on luminosity.
- Even ^{71}Ga experiments sensitve largely to high energy ν.

Solar Neutrinos IV

- Possible solutions to solar neutrino problem:
  - Standard solar model is incorrect (5-10% lower temperature in core gives neutrino flux consistent with Homestake detector).
  - Neutrino physics is incomplete (i.e. the standard model of particle physics is wrong!)
  - Nuclear physics describing the pp-chain is incorrect
  - Nuclear physics describing interaction between neutrino and ^{37}Cl is incorrect (Kamiokande & ^{71}Ga showed that this wasn't the problem)

Resolution of neutrino problem

- SNO (Sudbury Neutrino Observatory) in Sudbury, Canada uses D_2O and can detect not just the electron neutrino, but also μ and τ neutrinos

➔ The neutrinos aren't missing, e^- neutrinos produced in the Sun just convert into μ and τ neutrinos

➔ The problem lies with the neutrino physics.

- The neutrino has a small rest mass (10^{-8} m_e), which allows it to oscillate between the three flavours: e^- neutrino, μ neutrino and τ neutrino (proposed 1969 by russian theorists: Bruno Pontecorvo and Vladimir Gribov, … but nobody believed them)
- Confirmation by measuring anti-neutrinos from power plant (with Superkamiokande).

Resolution of neutrino problem II

- Lesson learnt: neutrinos have a multiple personality problem (J. Bahcall)
- Other lesson learnt: the "dirty" and difficult solar model turned out to be correct, the clean and beautiful standard theory of particle physics turned out to be wrong, or at least incomplete (J. Bahcall)
- 2002: Raymond Davis got Nobel prize for uncovering the neutrino problem

Standard solar model

- Ingredients: Conservation laws and material dependent equations
  - Mass conservation
  - Hydrostatic equilibrium (= momentum conservation in a steady state)
  - Energy conservation
  - Energy transport
  - Equation of state
  - Expression for entropy
  - Nuclear reaction networks and reaction rates → energy production
  - Opacity
- Assumptions: standard abundances, no mixing in core or in radiative zone, hydrostatic equilibrium, i.e. model passes through a stage of equilibria (the only time dependence is introduced by the reduction of H and the build up of He in the core).

Equations describing solar interior

Mass conservation :

$$\frac{\partial r}{\partial m} = \frac{1}{4\pi\rho r^2}$$

ρ = gas density

Hydrostatic equilibrium :

$$\frac{\partial P}{\partial m} = -\frac{Gm}{4\pi r^4}$$

P = pressure

G = Gravitational constant

Energy balance :

$$\frac{\partial L}{\partial m} = \varepsilon - T\frac{\partial S}{\partial T}$$

ε = energy generation per unit mass

T = temperature

S = entropy

Equation of state :

$\rho = \rho(P,T)$

or (for an ideal gas) :

$$P_G = \frac{\rho \Re T}{\mu}$$

P_G = gas pressure

$\Re$ = gas constant

μ = mean molecular weight

Energy transport :

$$F = F_R + F_C + F_{cond} = \frac{L}{4\pi r^2}$$

F = total energy flux

F_R = radiative flux

F_C = convective flux

F_{cond} = conductive flux

L = luminosity

Internal structure of the Sun

- Internal models shown for ZAMS Sun (subscript z) and for present day Sun (radius reaching out to 1.0, subscript ⊙)

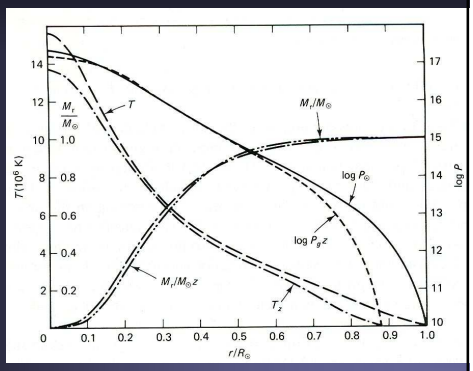

Solar evolution

- Path of the Sun in the HR diagram, starting in PMS stage and ending at
  - Red giant stage
  - White dwarf stage
- Note the complex patch during the red giant phase due to various phases of Helium burning and core contraction and expansion, etc.
- η ~ mass loss rate

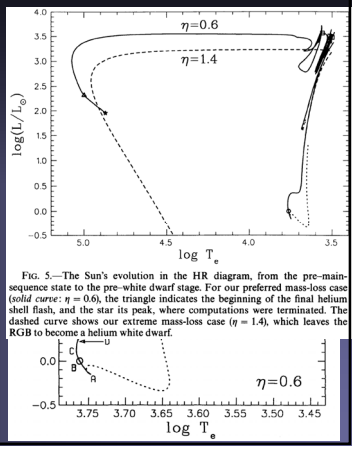

FIG. 5.—The Sun's evolution in the HR diagram, from the pre-main-sequence state to the pre-white dwarf stage. For our preferred mass-loss case (*solid curve*: $\eta = 0.6$), the triangle indicates the beginning of the final helium shell flash, and the star its peak, where computations were terminated. The dashed curve shows our extreme mass-loss case ($\eta = 1.4$), which leaves the RGB to become a helium white dwarf.

Evolution of Sun's luminosity

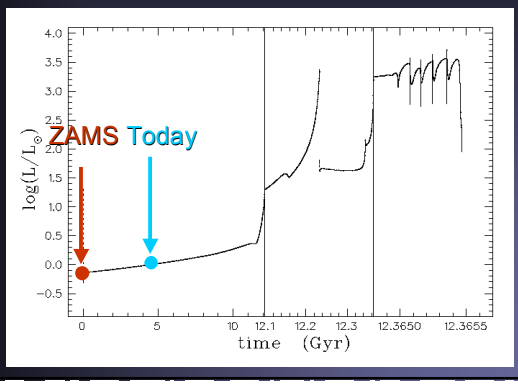

Faint young Sun paradox

- According to the standard solar model the Sun was approximately 30% less bright at birth than it is today
- Too faint to keep the Earth free of ice!
- Problem: Albedo of ice is so high that even with its current luminosity the Sun would not be able to melt all the ice away.
- Obviously the Earth is not covered with ice...
- So: Where is the mistake?

Possible resolution of the faint young Sun paradox

- The Earth's atmosphere was different 4 Gyr ago. More methane and other greenhouse gases. Higher insulation meant that even with lower solar input the Earth remained ice-free.
- As the Sun grew brighter life grew more abundant and changed the atmosphere of the Earth, reducing the greenhouse effect.
- Problem: what about Mars? Could it have had liquid water 4Gyr ago if Sun were so faint?
- Alternative: Sun was slightly more massive (1.04-1.07$M_\odot$) at birth and lost this mass (enhanced solar wind) in the course of time (Sackmann & Boothroyd 2003, ApJ). A more massive star on the ZAMS emits more light. Also agrees w. Mars data

Evolution of solar luminosity

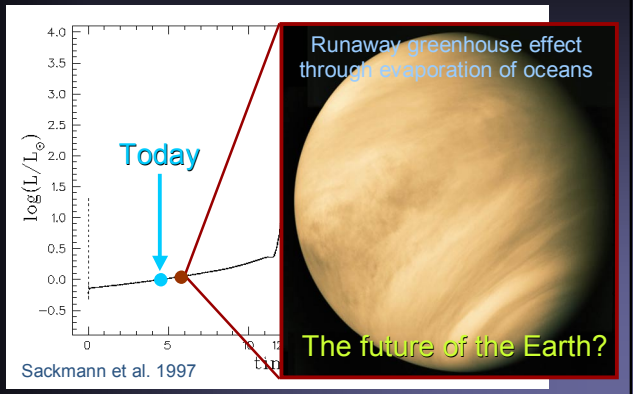

Sackmann et al. 1997

Solar radiation and spectrum

The Sun in white light: Limb darkening

- In the visible, the Sun's limb is darker than the centre of the solar disk (Limb darkening)
- Since intensity ~ Planck function, $B_\nu(T)$, T is lower near limb.
- Due to grazing incidence we see higher near limb: T decreases outward

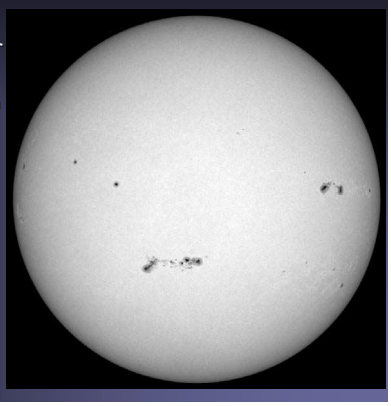

Limb darkening vs. λ

- Upper fig.:
  - short λ: large limb darkening;
  - long λ: small limb darkening
- departure from straight line: limb darkening is more complex than $I(\theta) \sim \cos(\theta)$

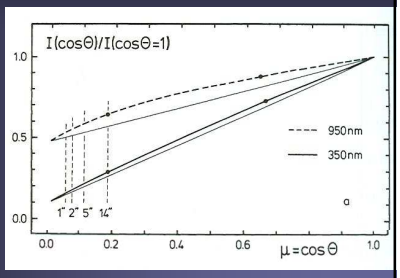

The Sun in the EUV: Limb brightening

- In the EUV, the Sun's limb is brighter than the centre of the solar disk (Limb brightening)
- Since the solar atmosphere is optically thin at these wavelengths, intensity ~ thickness of layer contributing to it. Due to geometrical effects this layer appears thicker near limb (radiation comes from roughly the same height everywhere).

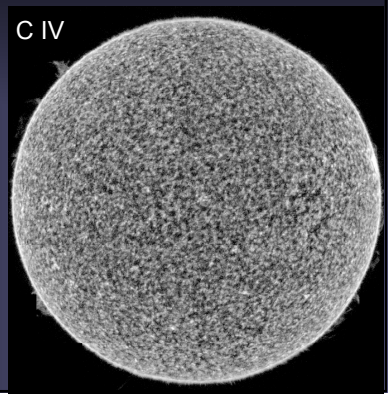

The Sun in the EUV: Limb brightening

- Limb brightening in optically thin lines does not imply that the Sun's temperature increases outwards (although by chance it does in these layers....)

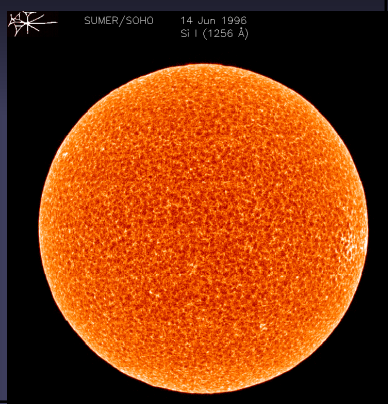

Solar irradiance spectrum

Irradiance = solar flux at 1AU

Spectrum is similar to, but not equal to Planck function ➔ Radiation comes from layers with diff. temperatures.

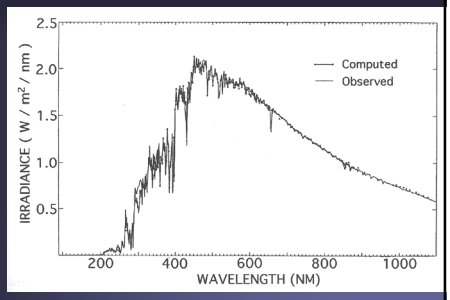

Often used temperature measure for stars: Effective temp: σT^4_{eff} = Area under flux curve

Absorption in the Earth's atmosphere

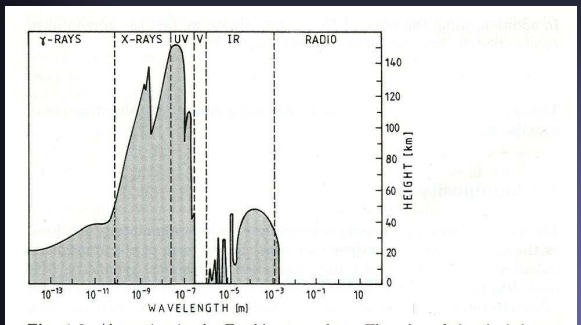

Fig. 1.2. Absorption in the Earth's atmosphere. The edge of the shaded area marks the height where the radiation is reduced to 1/2 of its original strength. UV ultraviolet; V visible; IR infrared

The solar spectrum: continua with absorption and emission lines

- The solar spectrum changes in character at different wavelengths.
- X-rays: Emission lines of highly ionized species
- EUV: Emission lines of neutral to multiply ionized species plus recombination continua
- UV: stronger recombination continua and absorption lines
- Visible: H^- b-f continuum with absorption lines
- FIR: H^- f-f continuum, increasingly cleaner (i.e. less lines, except molecular bands)
- Radio: thermal and, increasingly, non-thermal continua

Visible

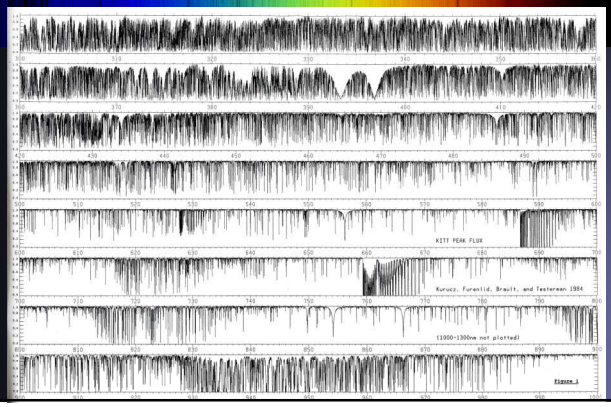

Solar UV spectrum

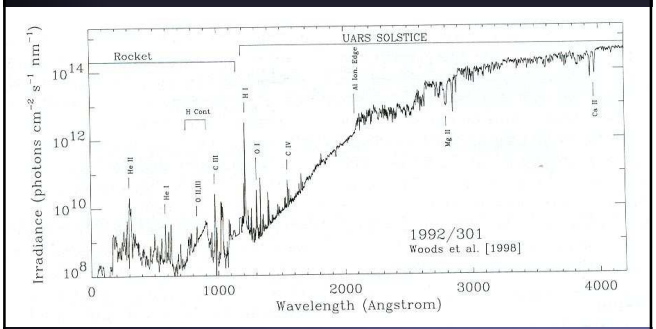

Note the transition from absorption lines (for λ>2000Å) to emission lines (for λ<2000Å)

EUV spectrum

- The solar spectrum from 500 Å to 1600 Å measured by SUMER (logarithmic scale)

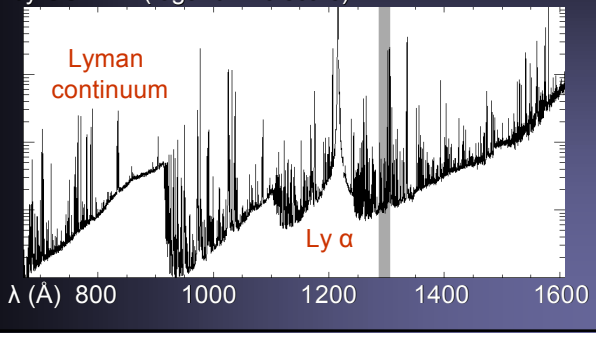

Detail of EUV spectrum by SUMER

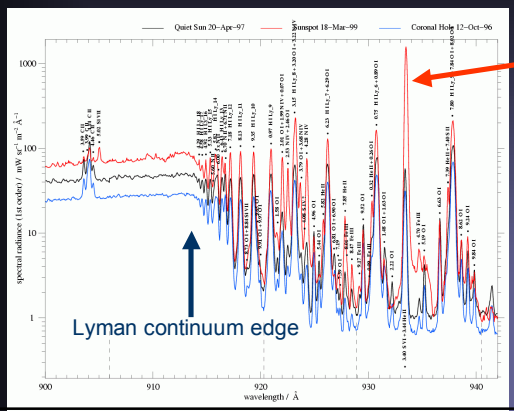

Activity sensitive line: S VI

Solar EUV irradiance

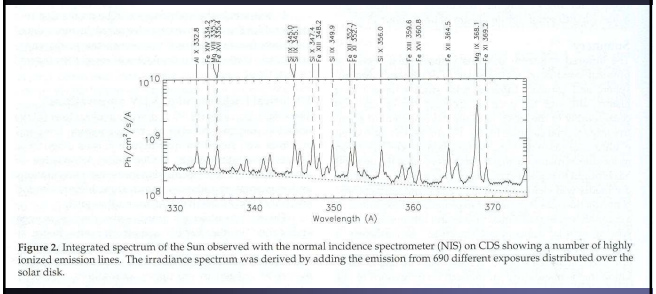

Figure 2. Integrated spectrum of the Sun observed with the normal incidence spectrometer (NIS) on CDS showing a number of highly ionized emission lines. The irradiance spectrum was derived by adding the emission from 690 different exposures distributed over the solar disk.

Formation of the solar spectrum

- Continuum
  - Spectral energy distribution
  - Centre to limb variation
- Spectral lines
  - Absorption lines
  - Emission lines
- Radiative transfer

Radiative transfer: optical depth

- Axis z points in the direction of light propagation
- Optical depth: $\Delta\tau_\nu = -\kappa_\nu \Delta z$

  where κ_ν is the absorption coefficient and ν is the frequency of the radiation. Light only knows about the τ_ν scale and is unaware of z

➔ Integration: $\tau_\nu = -\int \kappa_\nu(z) dz$

(note that the scales are floating, no constant of integration is fixed)

Optical depth and solar surface

- Radiation escaping from the Sun is emitted mainly at values of $\tau_\nu \approx 1$.
- At wavelengths at which κ_ν is larger, the radiation comes from higher layers in the atmosphere.
- In solar atmosphere κ_ν is small in visible and near IR, but large in UV and FIR ➔ We see deepest in visible and NIR, but sample higher layers at shorter and longer wavelengths.

Height of $\tau = 1$, brightness temperature and opacity vs. λ

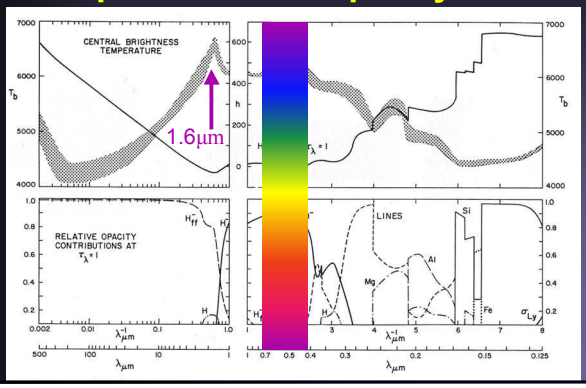

Radiative Transfer Equation

- Equation of radiative transfer:

  $\mu \, dI_\nu/d\tau_\nu = I_\nu - S_\nu$

  where I_ν is the intensity (i.e. the measured quantity) and S_ν is the source function. $\mu = \cos\theta$ is only important for non-vertical rays.
- S_ν = emissivity ε_ν divided by absorption coefficient κ_ν
- The physics is hidden in ε_ν and κ_ν, i.e. in τ_ν and S_ν.
- These quantities depend on temperature, pressure, elemental abundances, and frequency or wavelength

Formal solution of RT equation

- For $S_\nu = 0$ the solution of the RTE in a slab with (optical) boundaries $\tau_{\nu 2}$ and $\tau_{\nu 1}$ is :

$$I_\nu(\tau_{\nu 2}) = I_\nu(\tau_{\nu 1}) \exp(-\tau_{\nu 2} + \tau_{\nu 1})$$

- For general case formal solution reads (formal soln. assumes that we already know S_ν)

$$I_\nu(\tau_{\nu 2}) = I_\nu(\tau_{\nu 1}) \exp(-\tau_{\nu 2} + \tau_{\nu 1}) + \int S_\nu \exp(-\tau_\nu)\, d\tau_\nu$$

- 1st term describes radiation that enters through lower boundary (only absorption, no emission in slab), 2nd term describes radiation emitted in slab.
- In a stellar atmosphere $\tau_{\nu 1} = \infty$, so that only the 2nd term survives (lower boundary is unimportant).

When is an emission line formed, when an absorption line?

- Continua are formed deeper in a stellar atmosphere than spectral lines at the same wavelengths.
- A line is in absorption if S_ν decreases with height, i.e. if the absorption at greater heights dominates over emission
- A line is in emission if S_ν increases with height, i.e. if the emission at greater heights dominates over absorption

Statistical equilibrium

- In general both S_ν and κ_ν require a computation of the full statistical equilibrium for the species being considered.
- This implies computing how much each atomic/ionic/molecular level is populated, i.e. solving rate equations describing transitions to and from each considered level.
- Requires detailed knowledge of atomic, ionic, molecular structure and transitions.

The assumption of LTE

- In the solar interior and photosphere (i.e. where density is large and collisions are common) we can assume Local Thermodynamic Equilibrium (LTE)
- Thermodynamic equilibrium (TE): a single temperature everywhere (blackbody) ➔ Radiation emerging from object follows the Planck function B_ν.
- LTE: Each layer of the solar atmosphere has its own temperature ➔ Replace S_ν by $B_\nu(T)$ in the RTE and its solution.
- Problem of knowing S_ν is reduced to knowing $T(\tau)$ in the atmosphere.
- In addition, the statistical equilibrium can be solved simply by considering the Saha-Boltzmann equilibrium ➔ basically T and n_e need to be known.

Elemental abundances

- **Photospheric values**
- Logarithmic (to base 10) abundances of the 32 lightest elements on a scale on which H has an abundance of 12
- Heavier elements all have low abundances
- Note that in general the solar photospheric abundances are very similar to those of meteorites, with exception of Li, with is depleted by a factor of 100.

Element	Photosphere	Meteorites
1 H	12.00	–
2 He	10.93 ± 0.004	–
3 Li	1.10 ± 0.10	3.31 ± 0.04
4 Be	1.40 ± 0.09	1.42 ± 0.04
5 B	2.55 ± 0.30	2.79 ± 0.05
6 C	8.52 ± 0.06	–
7 N	7.92 ± 0.06	–
8 O	8.83 ± 0.06	–
9 F	4.56 ± 0.3	4.48 ± 0.06
10 Ne	8.08 ± 0.06	–
11 Na	6.33 ± 0.03	6.32 ± 0.02
12 Mg	7.58 ± 0.05	7.58 ± 0.01
13 Al	6.47 ± 0.07	6.49 ± 0.01
14 Si	7.55 ± 0.05	7.56 ± 0.01
15 P	5.45 ± 0.04	5.56 ± 0.06
16 S	7.33 ± 0.11	7.20 ± 0.06
17 Cl	5.5 ± 0.3	5.28 ± 0.06
18 Ar	6.40 ± 0.06	–
19 K	5.12 ± 0.13	5.13 ± 0.02
20 Ca	6.36 ± 0.02	6.35 ± 0.01
21 Sc	3.17 ± 0.10	3.10 ± 0.01
22 Ti	5.02 ± 0.06	4.94 ± 0.02
23 V	4.00 ± 0.02	4.02 ± 0.02
24 Cr	5.67 ± 0.03	5.69 ± 0.01
25 Mn	5.39 ± 0.03	5.53 ± 0.01
26 Fe	7.50 ± 0.05	7.50 ± 0.01
27 Co	4.92 ± 0.04	4.91 ± 0.01
28 Ni	6.25 ± 0.04	6.25 ± 0.01
29 Cu	4.21 ± 0.04	4.29 ± 0.04
30 Zn	4.60 ± 0.08	4.67 ± 0.04
31 Ga	2.88 ± 0.10	3.13 ± 0.02
32 Ge	3.41 ± 0.14	3.63 ± 0.04

Elemental abundances: the FIP effect

- In TR and corona abundances differ from photospheric values depending on the first ionization potential (FIP) of element.
- Elements with low FIP have enhanced abundance
- Apparently, acceleration through the chromosphere is more efficient for these elements (which are ionized in chromosphere, while high FIP elements are not).

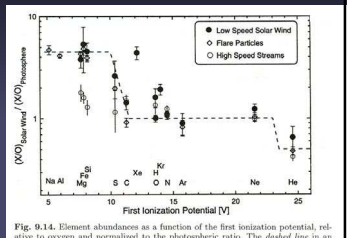

Fig. 9.14. Element abundances as a function of the first ionization potential, relative to oxygen and normalized to the photospheric ratio. The *dashed line* is an approximation to the slow-wind and flare-particle abundance ratios (except for Kr and Xe). From Geiss (1998)

Spectrum synthesis by 1-D radiative equilibrium model

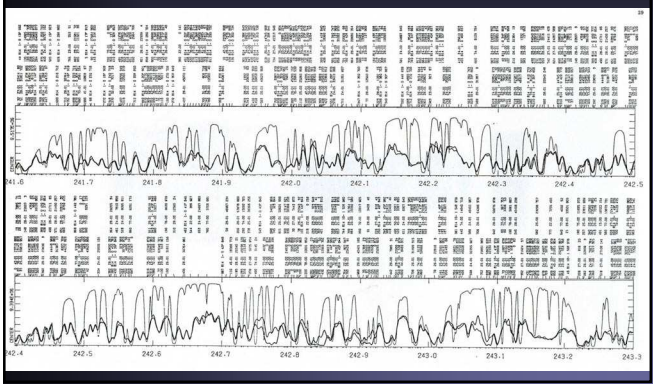

Diagnostic power of spectral lines

- Doppler shift of line: (net) flows in the LOS direction.
- Line width: temperature and turbulent velocity
- Equivalent width: elemental abundance, temperature (via ionisation and excitation balance)
- Line depth: temperature and temperature gradient
- Line asymmetry: inhomogenieties in the solar atmosphere.

Heights of formation: on which layers do lines give information ?

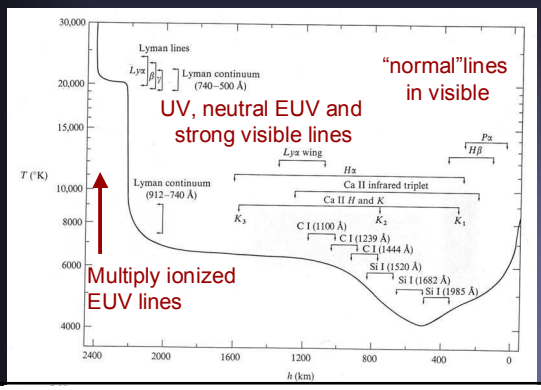

Solar convection

The convection zone

- Through the outermost 30% of solar interior, energy is transported by convection instead of by radiation
- In this layer the gas is convectively unstable. The unstable region ends just below the solar surface. I.e. the visible signs of convection are actually due to overshooting.
- Due to this, the time scale changes from the time scale for a random walk of the photons through the radiative zone (due to high density, the mean free path in the core is well below a millimeter) to the convective transport time:
- $t_{\text{radiative}} \sim 10^6$ years >> $t_{\text{convective}} \sim$ months

Scales of solar convection

- Observations: 4 main scales
  - **granulation**
  - mesogranulation
  - **supergranulation**
  - giant cells
- **Colour**:
  - **well observed**
  - less strong evidence
- Theory: larger scales at greater depths. In detail a lot is unclear.

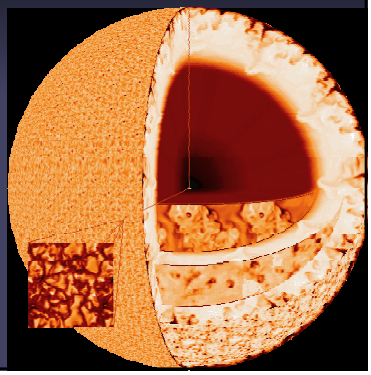

Surface convection: granulation

- Typical size: 2 Mm
- Lifetime: 6-8 min
- Velocities: 1 km/s (but peak velocities > 10 km/s, i.e. supersonic)
- Brightness contrast: 20% in visible continuum (under ideal conditions)
- All quantities show a continuous distribution of values
- At any one time 10^6 granules on sun.

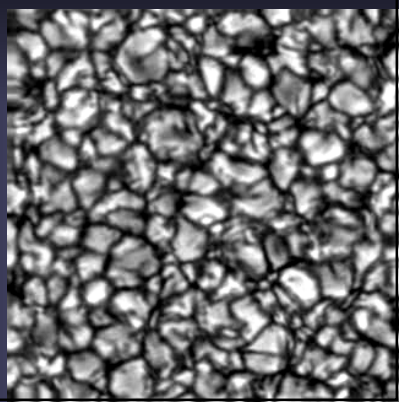

Surface convection: Supergranulation

- 1 hour average of MDI Dopplergrams (averages out oscillations).
- Dark-bright: flows towards/away from observer.
- No supergranules visible at disk centre: velocity is mainly horizontal
- Size: 20-30 Mm, lifetime: days, horiz. speed: 400 m/s, no contrast in visible

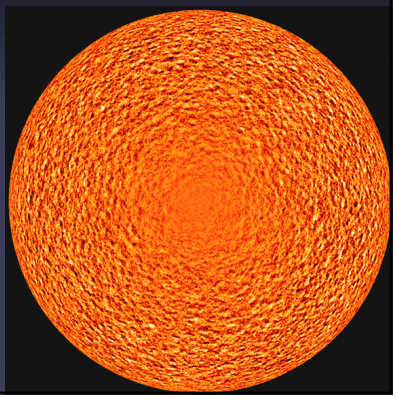

Observing convection

- Observing granulation
  - Continuum images and movies at high spatial resolution: gives sizes, lifetimes and evolution (splitting and dissolving granules), contrasts
  - Spectral lines (also at low spatial resolution). Line bisectors, line widths and convective blue shifts: contrasts, area factors, stratification
- Observing supergranulation
  - Images and movies in cores of chromospheric spectral lines, or magnetograms: observe the magnetic field at the edges of the supergranules instead of the supergranules directly
  - Helioseismic techniques

Line bisectors

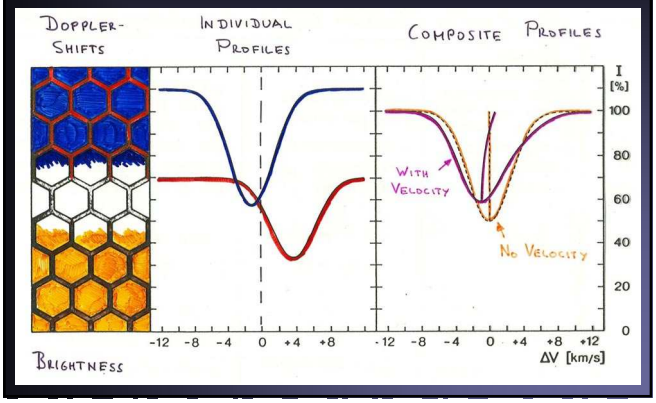

Supergranules seen by SUMER

- Si I 1256 Å full disk scan by SUMER in 1996
- Bright network indicates location of magnetic network
- Darker cells: supergranules

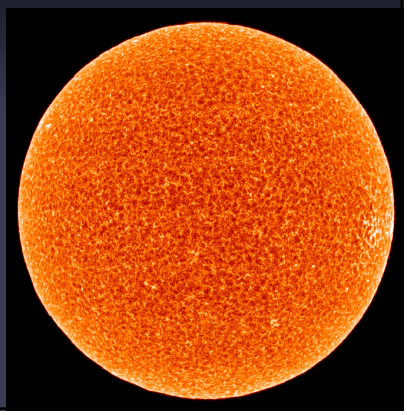

Supergranules & magnetic field

- Why are super-granules seen in chromospheric and transition region lines?
- Supergranules are related to the magnetic network.
- Network magnetic fields are concentrated at edges of supergranules.

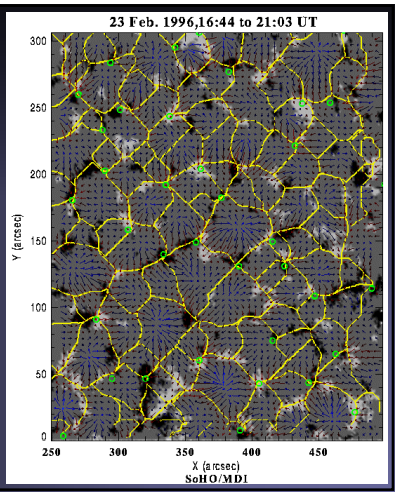

Illustration of convectively stable and unstable situations

Convectively stable

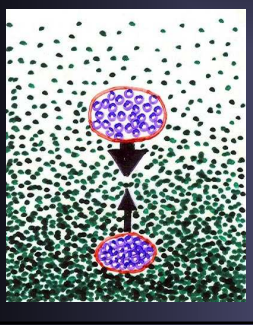

Convectively unstable

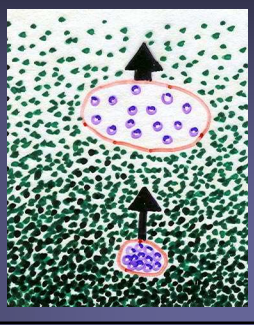

Onset of convection

Schwarzschild's instability criterion

Consider a rising bubble of gas:

ρ^*	ρ	$z-\Delta z$
ρ	$\rho_0 = \rho$	z
bubble	surroundings	depth

Condition for convective instability: $\rho^* < \rho_0$

For small Δz, bubble will not have time to exhange heat with surroundings: adiabatic behaviour. Convectively unstable if:

$$[d\rho/dz - (d\rho/dz)_{adiab}]\,\Delta z < 0$$

$d\rho/dz$: true stellar density gradient,

$(d\rho/dz)_{adiab}$: adiabatic gradient

Onset of convection II

Rewriting in terms of temperature and pressure:

$\nabla_{ad} = (d \log T / d \log P)_{ad}$

$\nabla_{rad} = (d \log T / d \log P)_{rad}$ = gradient in an atmosphere with radiative energy transport

Schwarzschild's convective instability criterion:

$$\nabla_{ad} < \nabla_{rad}$$

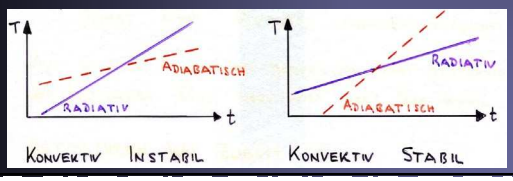

Why an outer convection zone?

- Why does radiative grad exceed adiabatic gradient?
- Mainly: radiative gradient becomes very large due to ionization of H and He below the solar surface.
- Expression for radiative gradient (for Eddington approximation):

  $\nabla_{rad} = (3F_r / 16\sigma g)(\kappa_{gr} P_g / T^4)$

  - F_r = radiative flux (≈ constant)
  - σ = Stefan-Boltzmann constant
  - g = gravitational acceleration (≈ constant)
  - κ_{gr} = absorption coefficient per gram. As H and He become ionized with depth, κ_{gr} increases rapidly, leading to large radiative gradient.

Ionisation of H and He

- Ionisation balance is described by Saha's equation: degree of ionisation depends on T and n_e
- H ionisation happens just below solar surface
- He → He^+ + e^- happens 7000 km below surface
- He^+ → He^{++} + e^- happens 30'000 km below surface
- Since H is most abundant, it provides most electrons (largest opacity) and drives convection most strongly
- At still greater depth, other elements also provide a minor contribution.

Radiative, adiabatic & actual gradients

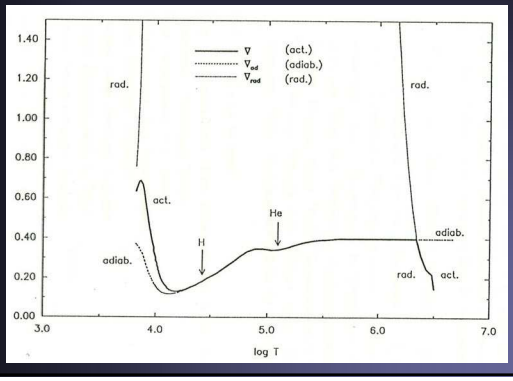

The mixing length

- As a gas packet rises, diffusion of particles and thermal exchange with surroundings causes it to lose its identity and to stop from moving on.
- Length travelled up to that point: mixing length l.
- Often used parameterization of l: $l = \alpha H_p$
  - H_p = pressure scale height
  - α = mixing length parameter, typically 1-2 (determined empirically)

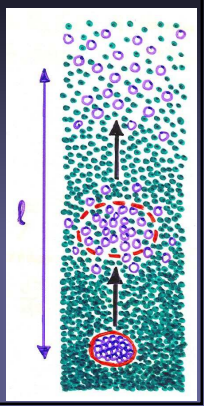

Why is mixing length interesting

- Gives an idea of the size scale of a convection cell (height or depth of cell given by mixing length)
- horizontal extent of cell cannot be much bigger than mixing length due to mass conservation!

History of mixing length

- Mixing length was introduced by L. Prandl, who was director at Max Planck Institut für Strömungsforschung in Göttingen.
- It allowed him to describe convection in a simple, but powerful way.
- Even today, most stellar interior models (and many atmospheric models) use the mixing length to describe the effects of convection.

Convective overshoot

- Due to their inertia, the packets of gas reaching the boundary of the CZ pass into the convectively stable layers, where they are braked & finally stopped.

➔overshooting convection

- Typical width of overshoot layer: order of H_p
- This happens at both the bottom and top boundaries of the CZ and is important:
  - top boundary: Granulation is overshooting material. $H_p \approx$ 100 km in photosphere
  - bottom boundary: the overshoot layer allows B-field to be stored → seat of the dynamo?

Convection simulations

- 3-D hydrodynamic simulations reproduce a number of observations and provide new insights into solar convection.
- These codes solve for mass conservation, momentum conservation (force balance, Navier-Stokes equation), and energy conservation including as many terms as possible.
- Problem: Simulations can only cover 2-3 orders of magnitude in length scale (due to limitations in computing power), while the physical processes on the Sun act over at least 6 orders of magnitude.
- Also, simulations can only cover a part of the size scale of solar convection, either granulation, supergranulation, or larger scales, but not all.

Convection simulations II

- Simulations do not achieve the solar Reynolds number ($R_e = vl/\nu$) of 10^{10} , where v = typical velocity, l = typical length scale, ν = kinematic viscosity (R_e ~ ratio of viscous to advection time scales).
- For comparison with observations it is important that the simulations describe the surface layers well, i.e. code needs to consider:
  - radiative transport of energy. Only few simulation codes do this properly.
  - partial ionization of many elements
  - as low a viscosity as numerically possible
- The role of radiation is primarily to transport energy. At the solar surface the energy transported by radiation becomes comparable to that by convection.

Simulations of solar granulation

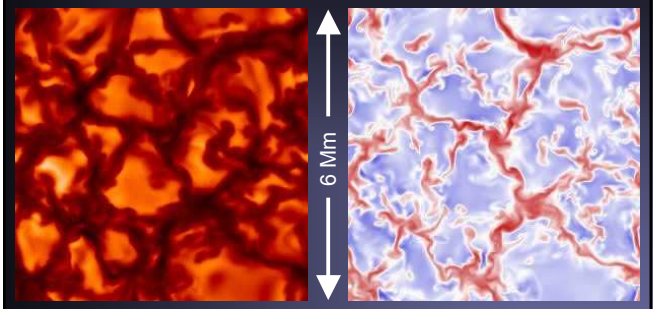

Solution of Navier-Stokes equation etc. describing fluid dynamics in a box (6000 km^2 x 1400 km) containing the solar surface. Realistic looking granulation is formed.

Testing the simulations

Comparison between observed and computed bisectors for selected spectral lines (2 computed bisectors shown: one each with and without oscillations in the atmosphere)

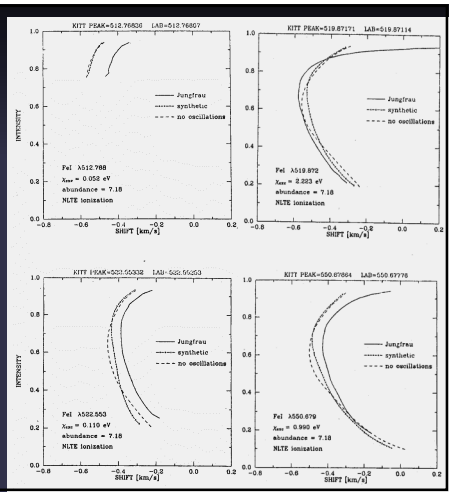

Granule structure

Upflows are broad & slow, downflows are narrow and fast. Why?

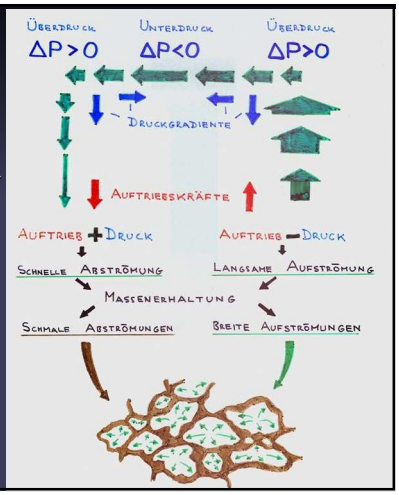

Granule evolution

- Granules die in two ways:
  - dissolve: grow fainter and smaller until they disappear (small granules)
  - split: break into two smaller granules (large granules)
- Granules are born in two ways:
  - as fragments of a large splitting granule
  - appearing as small structures and growing
- Initially most granules grow in size, some keep growing until they become unstable (see next slide) and split, others stop growing and start shrinking until they disappear (all within 5-10 min).

Granule evolution II

- Why do large granules split and small granules get squeezed out of sight?
- Granules are overshooting convection structures, with an upflow in their centre, a radial horizontal flow over the whole granule and a downflow in the surrounding lanes.
- The upflow builds up density and excess pressure above the granule → pressure gradient relative to flanks of granule.
- Pressure gradient = force.

→ Gas is accelerated sideways.

- Above intergranular lane: horizontally flowing gas meets gas from opposite granule → build up pressure excess which decelerates flow.

Granule evolution III

- Consider mass conservation: A larger granule will build up a larger pressure above its centre because more mass needs to be accelerated horizontally.
- At some point the pressure becomes so large that the upflow is quenched. The centre of the granule cools and a new downflow lane forms there. The granule splits

Relation between granules and supergranules

- Downflows of granules keep going down to bottom of simulations. However, the intergranular lanes break up into individual narrow downflows.
- I.e. topology of flow reverses with depth:
  - At surface: isolated upflows, connected downflows
  - At depth: connected upflows, isolated downflows
- Idea put forward by Spruit et al. 1990: At increasingly greater depth the narrow downflows from different granules merge, forming a larger and less fine-meshed network that outlines the supergranules.

Increasing size of convective cells with depth

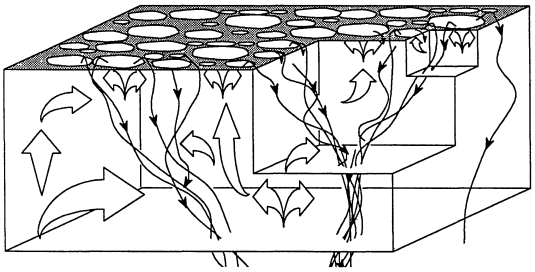

Figure 7 Flow lines showing the merging of the downdrafts on successively larger scales (schematic). The boxes cut out illustrate how the same process occurs on (in this illustration) three different scales.

Convection on other stars

- F, G, K & M stars posses outer convection zones and show observable effects of convection (also WDs)
- Observations are difficult since surfaces cannot be resolved.

➔Use line bisectors: independent of spatial resolution

- A,F stars show inverse bisectors: granulation has different geometry.

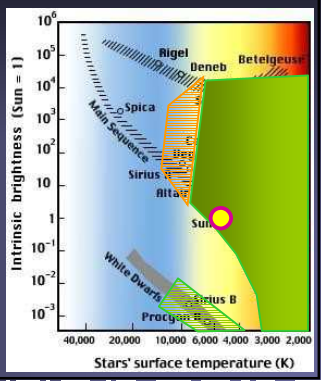

Oscillations and helioseismology

5-minute oscillations

- The entire Sun vibrates from a complex pattern of acoustic waves, with a period of around 5 minutes
- The oscillations are best seen as Doppler shifts of spectral lines, but also as intensity variations.
- Identified as acoustic waves, called p-modes
- Spatio-temporal properties of oscillations best revealed by 3-D Fourier transforms.

Doppler shift

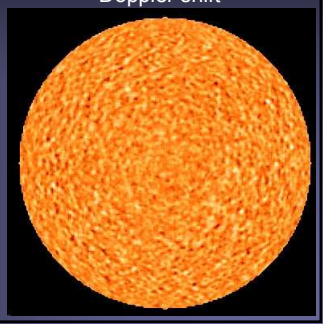

Solar Eigenmodes

- The p-modes show a distinctive dispersion relation (k-ω diagram: $k \sim \omega^2$)
- Important: there is power only in certain ridges, i.e. for a given k^2 ($= k_x^2 + k_y^2$), only certain frequencies contain power.
- This discrete spectrum suggests the oscillations are trapped, i.e. eigenmodes of the Sun.

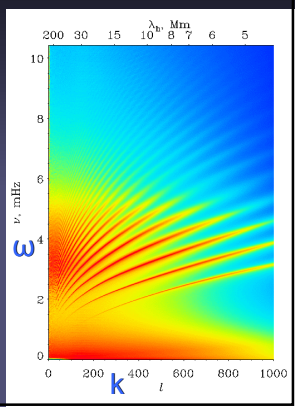

Global oscillations

- The Sun's acoustic waves bounce from one side of the Sun to the other, causing the Sun's surface to oscillate up and down. They are reflected at the solar surface.
- Modes differ in the depth to which they penetrate: they turn around because sound speed ($C_S \sim T^{1/2}$) increases with depth (refraction)
- p-modes are influenced by conditions inside the Sun. E.g. they carry info on sound speed
- By observing these oscillations on the surface we can learn about the structure of the solar interior

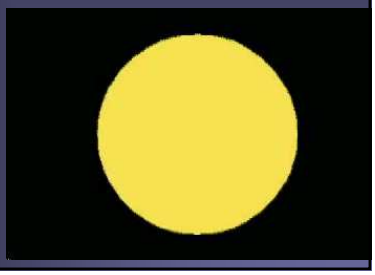

Description of solar eigenmodes

- Eigen-oscillations of a sphere are described by spherical harmonics
- Each oscillation mode is identified by a set of three parameters:
  - n = number or radial nodes
  - l = number of nodes on the solar surface
  - m = number of nodes passing through the poles (next slide)

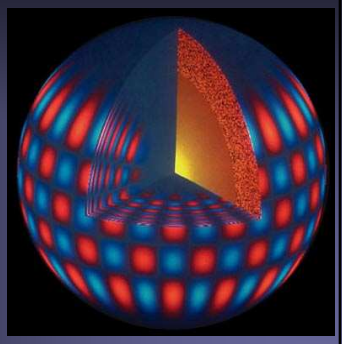

Illustration of spherical harmonics

- l = total number of nodes (in images: $l = 6$) = degree
- m = number of nodes connecting the "poles"

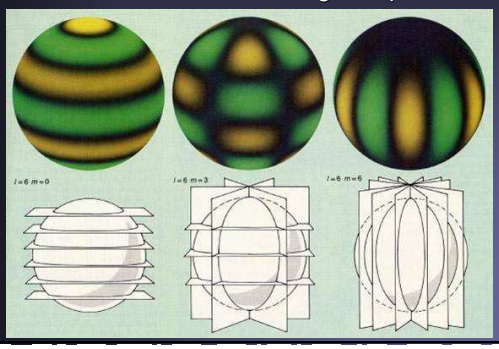

Spherical harmonics

- Let $v(\theta,\varphi,t)$ be the velocity, e.g. as measured at the solar surface over time t. Then:

$$v(\theta,\varphi,t) = \sum_{l=0}^{\infty} \sum_{m=-l}^{l} a_{lm}(t)\, Y_l^m(\theta,\varphi)$$

- The temporal dependence lies in a_{lm}, the spatial dependence in the spherical harmonic Y_l^m.

$$Y_l^m(\theta,\varphi) = P_l^{|m|}(\theta)\exp(im\varphi)$$

$$P_l^{|m|}(\theta) = \text{associated Legendre Polynomial}$$

- Due to the normalization of the spherical harmonic, the Fourier power is given by $F(a)F(a)^*$
- Here $F(a)$ is the Fourier transform of the amplitude a_{lm}

More examples and a problem with identifying spherical harmonics

- General problem: Since we see only half of the Sun, the decomposition of the sum of all oscillations into spherical harmonics isn't unique.
- This results in an uncertainty in the deduced l and m

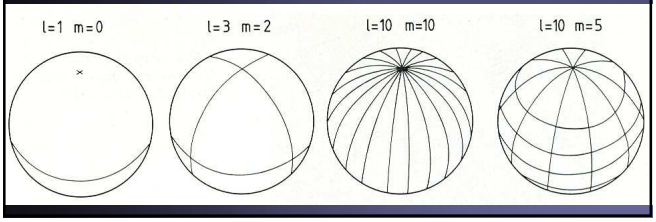

Interpretation of k-ω or ν-l diagram

- At a fixed l, different frequencies show significant power. Each of these power ridges belongs to a different order n (n = number of radial nodes), with n increasing from bottom to top.
- Typical are small values of n, but intermediate to large degree l.

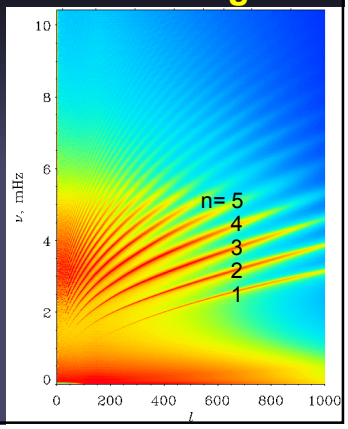

A few observational remarks

- 10^7 modes are present on the surface of the Sun at any given time (and interfering with each other).
- Typical amplitude of a single mode: < 20 cm/s
- Total velocity of all 10^7 modes: a few 100 m/s
- Accuracy of current instruments: better than 1 cm/s
- Frequency resolution ~ length of time series (Heisenberg's uncertainty principle) ~ lowest detectable frequency

➔ Longer time series are better

- Gaps in time series produce side lobes (i.e. spurious peaks in the power spectrum)
- Highest detectable frequency ~ cadence of obs.

Accuracy of frequency measurements

- Plotted are identified frequencies and error bars (yellow; 1000σ for blue freq., 100σ for red freq. below 5 mHz and 1σ for higher freq.)
- Best achievable freq. resolution: a few parts in 10^5; limit set by mode lifetime ~100 d

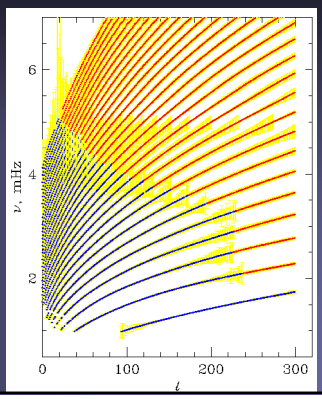

Frequency vs. amplitude

- Frequencies are the important parameter, more so than the amplitudes of the modes or of the power peaks.
- The amplitudes depend on the excitation, while the frequencies do not. They carry the main information on the structure of the solar interior.
- p-modes are excited by turbulence, which excites all frequencies. However, only at Eigenfrequencies of the Sun can eigenmodes develop.
- Frequencies (being more constant) are also measured with greater accuracy.

The measured low-l eigenmode signal

- Sun seen as a star: Due to cancellation effects, only modes with l=0,1,2 are visible ➔ simpler power spectrum.
- Low l modes are important for 2 reasons:
  - They reach particularly deep into the Sun (see cartoon on earlier slide).
  - These are the only modes measurable on other Sun-like stars.
- These modes are sometimes called "global" modes.
- The different peaks of given l correspond to different n values (n=15...25 are typical).

Best current low-l power spectrum

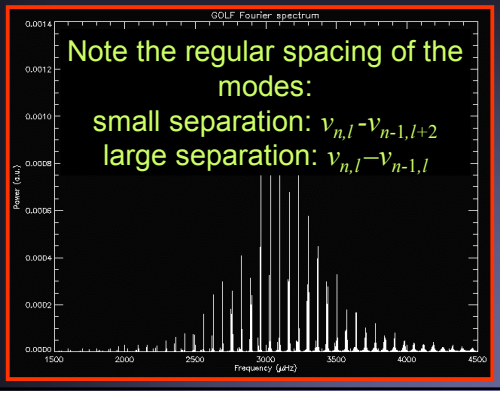

Mode structure of low l spectrum

- GOLF/SOHO observations showing a blowup of the power spectrum with an $l = 0$ and an $l = 2$ mode.
- The noise is due to random re-excitation of the oscillation mode by turbulence

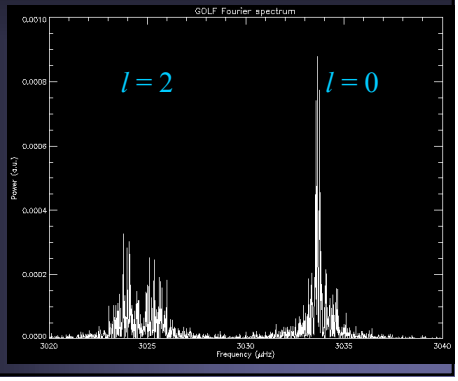

Types of oscillations

- Solar eigenmodes can be of 2 types:
  - p-modes, where the restoring force is the pressure, i.e. normal sound waves
  - g-modes, where the restoring force is gravity (also called buoyancy modes)
- So far only p-modes have been detected on the Sun with certainty.
- They are excited by the turbulence associated with the convection, mainly the granulation near the solar surface (since there the convection is most vigorous).
- Being p-modes, they travel with the sound speed C_S. They dwell longest where C_S is lowest. Since $C_S \sim T^{1/2}$, this is at the solar surface.

p-modes vs. g-modes

- p-modes propagate throughout the solar interior, but are evanescent (later slide) in the solar atmosphere
- g-modes propagate in the radiative interior and in the atmosphere, but are evanescent in the convection zone (their amplitude drops exponentially there, so that very small amplitudes are expected at the surface). Convection means buoyancy instability; oscillations require stability.
- g-modes are expected to be most sensitive to the very core of the Sun, while p-modes are most sensitive to the surface
- Current upper limit on solar interior g-modes lies below 1 cm/s.

Solar oscillations: simple treatment

- Equations describing radial structure of adiabatic oscillations, neglecting any perturbations to the gravitational potential, are:

$$\frac{1}{r^2}\frac{d}{dr}(r^2\xi_r) - \frac{\xi_r}{c^2} + \frac{1}{\rho_0}\left(\frac{1}{c^2} - \frac{l(l+1)}{r^2\omega^2}\right)P_1 = 0$$

$$\frac{1}{\rho_0}\frac{dP_1}{dr} + \frac{g}{\rho_0 c^2}P_1 - \left(\omega^2 - N^2\right)\xi_r = 0$$

$$\text{where } N^2 = g\left(\frac{1}{\Gamma P_0}\frac{dP}{dr} - \frac{1}{\rho_0}\frac{d\rho_0}{dr}\right) = \text{Brunt - Vaisala frequency}$$

- Here ξ_r is radial displacement and P_1 is pressure perturbs. Quantities with subscript 0 refer to the unperturbed Sun. Γ is the adiabatic exponent: $\Gamma = \left(\frac{d\ln P}{d\ln \rho}\right)$

Solar oscillations: simplified treatment II

- Analytical solutions of these equations for an isothermal atmosphere are readily obtained:

$$\xi_r(r) \sim \rho_0^{-1/2}\exp(ik_r r)$$

$$P_1(r) \sim \rho_0^{1/2}\exp(ik_r r)$$

- These oscillations are trapped in the body of the Sun. Since the time scale on which the atmosphere reacts to disturbances is low, waves which are travelling in the solar interior are evanescent in the atmosphere → They are present only for discrete frequencies (similar to the bound states in atomic physics).

Regimes of oscillation

- In regimes of acoustic and gravity waves $k_r^2 > 0$, while in regime of evanescent waves $k_r^2 < 0$ (exponential damping). The solid lines show $k_r^2 = 0$.
- Evanescent waves occur when the period is so long that the whole (exponentially stratified) medium has time to adapt to the perturbation, achieving a new equilibrium. Therefore the wave does not propagate, but rather the medium as a whole oscillates.

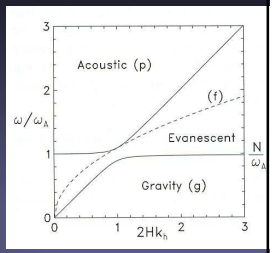

Cutoff frequency for acoustic waves in a stratified medium: $\omega_C = C_S/2H$

Deducing internal structure from solar oscillations

- Global helioseismology: Gives mainly the radial dependence of solar properties, although latitudinal dependence can also be deduced (ask R. Mecheri).
  - Radial structure of sound speed
  - Structure of differential rotation
- Local helioseismology: Allows in principle 3-D imaging of solar interior. E.g. time-distance helioseismology does not measure frequencies, but rather the time that a wave requires to travel a certain distance (relatively new)

Global helioseismology

- Use frequencies of many modes.
- Basically two techniques for deducing information on the Sun's internal structure
  - Forward modelling: make a model of the Sun's internal structure (e.g. standard model discussed earlier), compute the frequencies of the eigenoscillations of the model and compare with observations
  - Inverse technique: Deduce the sound speed and rotation by inverting the oscillations (i.e. without any comparison with models)
- Note that forward modelling is required in order to first identify the modes. Only after that can inversions be carried out.

Testing the standard solar model: results of forward modelling

- Relative difference between C_S^2 obtained from inversions and from standard solar model plotted vs. radial distance from Sun centre.
- Typical difference: 0.002 ➔ good!
- Typical error bars from inversion: 0.0002 ➔ poor!
- Problem areas:
  - solar core
  - bottom of CZ
  - solar surface

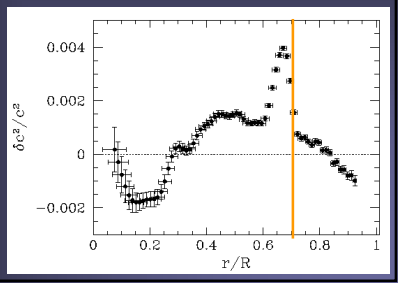

Variation of the solar rotation velocity with period of 1.3 years

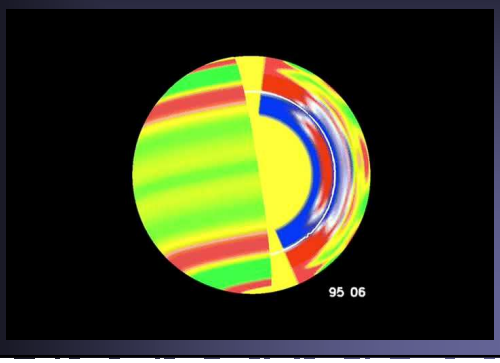

Local excitation of wave by a flare

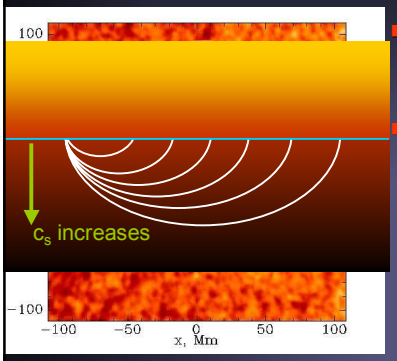

- Clear example of wave being triggered.
- The wave is not travelling at the surface, but rather reaching the surface further out at later times. Note how it travels ever faster. Why?

Local helioseismology

- Does not build upon measuring frequencies of eigenmodes, but rather measures travel times of waves through the solar interior, between two "bounces" at the solar surface (for particular technique of time-distance helioseismology).
- The travel time between source and first bounce depends on the structure of C_S below the surface. By considering waves following different paths inhomogeneous distributions of C_S can be determined.

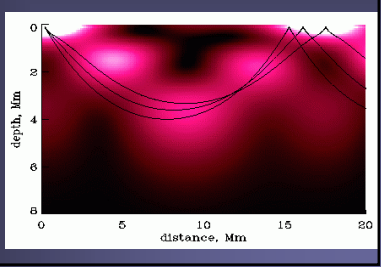

Local helioseismology II

- Temperature and velocity structures can be distinguished, since a flow directed with the wave will affect it differently than a flow directed the other way (increase/decrease the sound speed).
- By considering waves passing in both directions it is possible to distinguish between T and velocity.
- At right: 1st images of convection zone of a star!

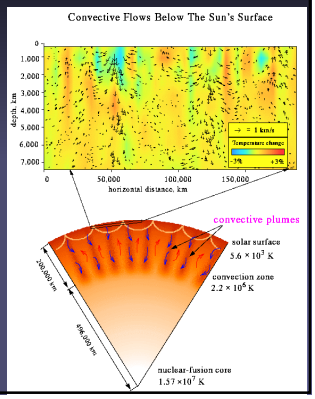

Time-Distance Helioseismology of a sunspot

- Subsurface structure of sunspots
- Sunspots are good targets, due to the large temperature contrast.
- Major problem: unknown influence of the magnetic field on the waves.

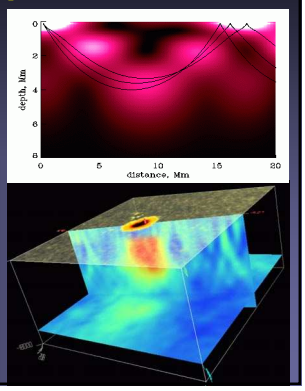

Time-Distance Helioseismology of a sunspot II

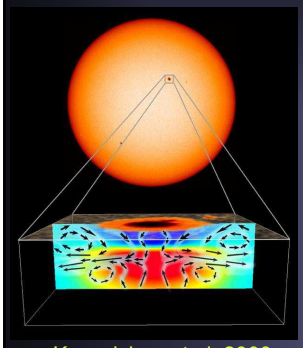

Kosovichev et al. 2000

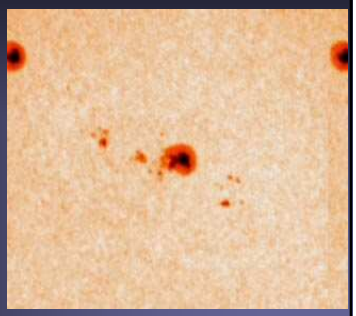

Zhao et al. 2004

Subsurface Structure of Sunspots

- How can sunspots last for several weeks without flying apart?
- Models: inflows
- Observations at surface: outflows (moat flow)

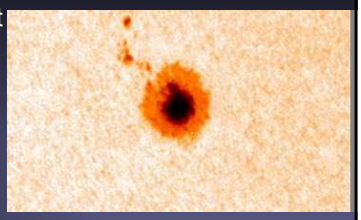

Zhao et al.: 2001, ApJ 557, 384

- Strong inward flows right underneath the surface
- Sunspots surprisingly shallow: become warmer than surroundings already some 4000 km below surface
- Results to be confirmed (unkown influence of B)

Seeing right through the Sun

- A technique, called two-skip far-side seismic holography, allows images of the far side of the Sun to be made.
- Waves from front go to back and then return.
- Acoustic waves speed up in active regions (hotter in subsurface layers)
- The delay of the sound waves is about 12 sec in a total travel time of 6 hours

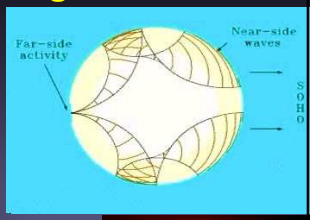

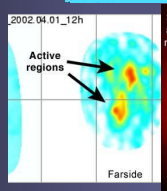

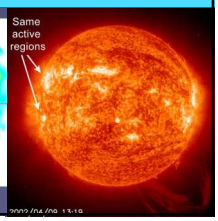

Seeing right through the Sun II

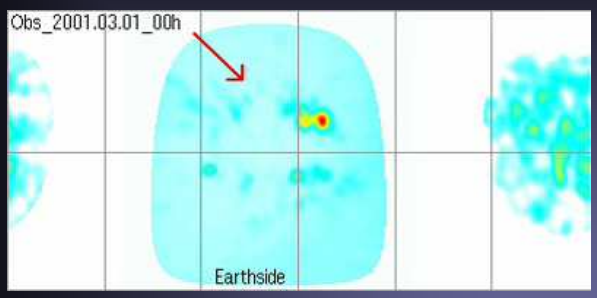

Real-time far side images:
http://soi.stanford.edu/data/farside/index.html

Helioseismology instruments

- Needed:
  - uninterrupted, long time series of observations
  - Either high velocity sensitivity, or high intensity sensitivity (and extremely good stability)
  - Low noise
  - Spatial resolution better than 1" (for local helioseismology)
- Instruments are either:
  - Ground based global networks (GONG+, BiSON)
  - Space based instruments in special full-Sun orbits (advantage of lower noise relative to ground-based networks; MDI, GOLF, VIRGO on SOHO, HMI on SDO)
  - Usually filter instruments with high spectral or intensity fidelity

Instruments and projects

- Ground (networks of 3 or more telescopes aimed at reducing the length and number of data gaps)
  - GONG+
  - BISON
  - TON
- Space (uninterrupted viewing, coupled with lack of noise introduced by the atmosphere)
  - SOHO MDI, GOLF and VIRGO (running)
  - SDO HMI (being built)
  - Solar Orbiter VIM (planned)

Asteroseismology

First reliable detection of oscillations on the near solar analogue, α Centauri, and other Sun-like stars. Note the shift in the p-mode frequency range to lower values for α Centauri, which is older than the Sun (note also factor 10^3 difference in ν scale)

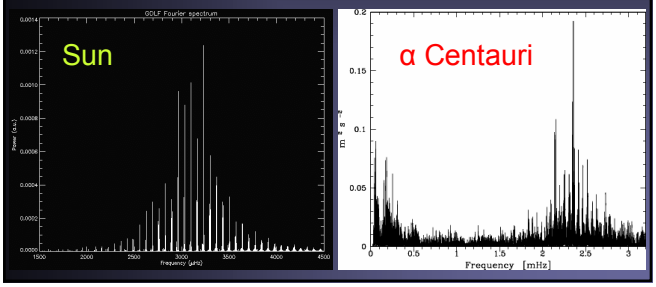

Projects

- Major asteroseismic Space missions:
  - COROT
  - Kepler
- Ground based:
  - ESO 3.6m (HARPS)
  - ESO VLT (UVES)
  - Networks of smaller Telescopes

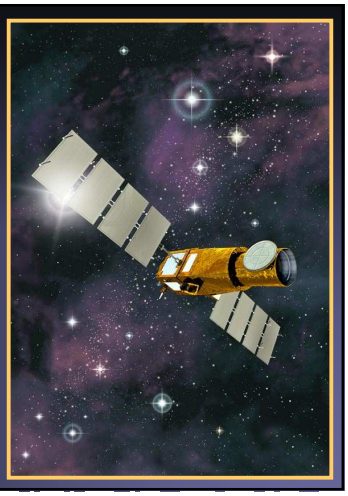

Solar rotation

Solar rotation

- The Sun rotates differentially, both in latitude (equator faster than poles) and in depth (more complex).
- Standard value of solar rotation: Carrington rotation period: 27.2753 days (the time taken for the solar coordinate system to rotate once).
- Sun's rotation axis is inclined by 7.1° relative to the Earth's orbital axis (i.e. the Sun's equator is inclined by 7.1° relative to the ecliptic).

Discovery of solar rotation

- Galileo Galilei and Christoph Scheiner noticed already that sunspots move across the solar disk in accordance with the rotation of a round body
- ➔ Sun is a rotating sphere
- Movie based on Galileo Galilei's historical data

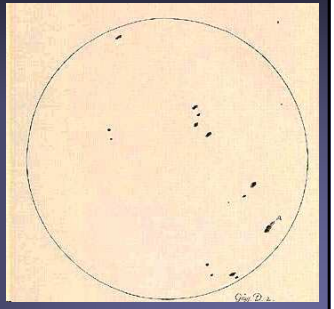

Surface differential rotation

- Poles rotate more slowly than equator.
- Surface differential rotation from measurements of:
  - Tracers, such a sunspots or magnetic field elements (always indicators of the rotation rate of the magnetic field)
  - Doppler shifts of the gas
  - Coronal holes (not plotted) rotate rigidly

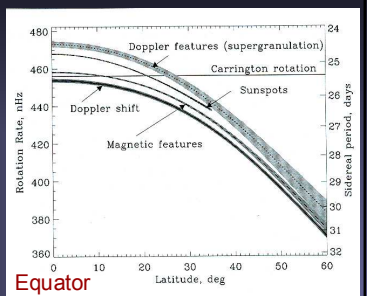

Figure 1. Rotation rate, $\Omega/2\pi$, and period of various tracers on the Sun's surface: recurrent (old) sunspots (dashed curve), magnetic features (dot–dash), and Doppler features (dots). The rotation rate and period determined spectroscopically through the Doppler shift are shown by the full curve. The shaded areas show the 1σ error estimates.

Surface differential rotation

- Description:

  $\Omega = A + B \sin^2\psi + C \sin^4\psi$

  where ψ is the latitude, $A = \Omega$ at the equator and $A+B+C = \Omega$ at the poles.
- Different tracers give different A, B, C values. E.g. spots rotate faster than the surface gas.

How come different rotation laws?

- Are different tracers anchored at different depths in the convection zone?
  - Evidence in support comes from sunspots: young spots rotate faster than older spots (→ older spots are slowed down by the surrounding gas)
- How come coronal holes rotate rigidly, while the underlying photospheric magnetic field rotates differentially?
  - ➔Individual magnetic features must move in and out of coronal holes
  - ➔Support: evidence for enhanced magnetic reconnection at the edges of coronal holes

Internal differential rotation

- Method: Helioseismic inversions
  - In a non-rotating star the individual modes of oscillation, described by "quantum numbers" n,l,m are degenerate in that their frequency depends only on n and l, but not on m.
  - Similar to Zeeman effect. Note that m distinguishes between the surface distribution of oscillation nodes. For a spherically symmetric star (no rotation) all these modes must have same frequency.
  - In a rotating Sun the degeneracy is removed and modes with different m have slightly different frequency.
  - Since modes with different l sample the solar latitudes in different ways, it is possible to determine not just vertical, but also latitudinal differential rotation by helioseismology.

Internal differential rotation II

- Structure of internal rotation deduced from MDI data
- Note: differential rotation in CZ, solid rotation below

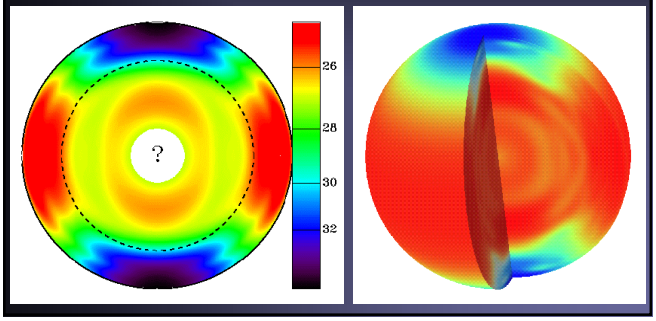

Internal differential rotation III : tachocline

Large radial gradients in rotation rate at bottom of CZ (tachocline), but also just below solar surface (enigmatic). Note the slight missmatch of helio-seismic and Doppler measurements

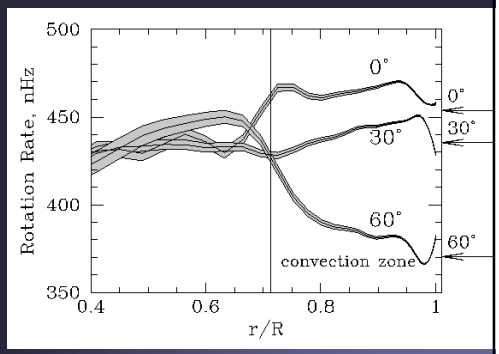

What about rotation of solar core?

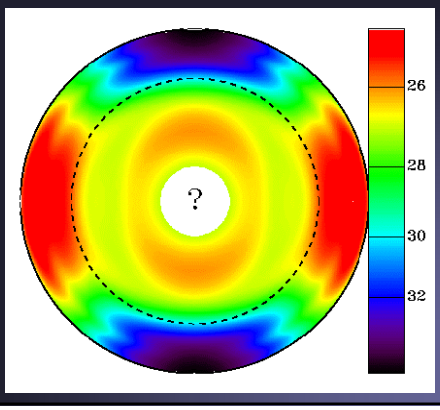

What about rotation of solar core?

- Rotation rate of solar core is not easy to determine, since p-modes are rather insensitive to the innermost part of the Sun.
- Different values in the literature for the core's rotation rate: $\Omega(r=0) = \Omega(r=R_\odot)$ … $2\,\Omega(r=R_\odot)$
- One way to set limits on $\Omega(r=0)$: quadrupole moment of Sun.
- Solar rotation leads to oblateness, i.e. diameter is larger at equator than between the poles.
- If core rotates more rapidly than surface, then oblateness will be larger than expected due to surface rotation rate.

Solar oblateness

- Oblateness = $\Delta R/R_\odot$
- Direct measurements: $\Delta R/R_\odot \approx 10^{-5}$
  - Very tricky, since oblateness 10^{-5} corresponds to ΔR = 14 km (best spatial resolution achievable: 100 km).
  - Systematic errors due to concentration of magnetic activity to low latitudes → affects measurements of solar diameter, since shape of limb is distorted.
  - Initial measurements due to Dicke & Goldenberg (1967) gave $\Delta R/R_\odot \approx 5\times10^{-5}$ → required change of general relativity to explain motion of Mercury's perihelion (but was consistent with Brans-Dicke gravitation theory)
- Helioseismic measurements give for the acoustic radius of the Sun (which is not the same as the optical radius, but similar): $\Delta R/R_\odot \approx 10^{-5}$ (Redouane Mecheri)

Evolution of solar rotation

- Young stars are seen to rotate up to 100 times faster than the Sun.
- Did the Sun also rotate faster when it was young?
- Skumanich law: $\Omega \sim t^{-1/2}$, where t is the age of the star (deduced from observing stars in clusters of different ages).

➔Sun also rotated faster as a young star.

- Question: where did all the angular momentum go?

Evolution of solar rotation II

- Question: where did all the angular momentum go?
- Answer part 1: Solar wind! The solar wind carries away angular momentum with it. Torque j, i.e. rate of change in angular momentum, exerted by solar wind (without magnetic field):

$$j = \Omega R_\odot dm/dt$$

- Here dm/dt is the solar mass-loss rate (mass carried away by solar wind)
- Problem: j is 2-3 orders of magnitude too small to cause a significant braking of solar rotation…

Evolution of solar rotation III

- Answer part 2: Magnetic field!
- Solar wind is channeled by magnetic field up to the Alfven radius R_A, i.e. point where wind speed > Alfven speed. Up to that radius, the wind rotates rigidly with the solar surface (forced to do so by rigid field lines), i.e. it only carries angular momentum away beyond R_A. Proper expression for Torque:

$$j = \Omega R_A dm/dt$$

- R_A typically is 10-20 times larger than $R_\odot$.

Evolution of rotation IV

- $j = \Omega R_A dm/dt \sim \Omega$

➔The faster the star rotates, the quicker it spins down.

- Additional corrections:
  - dm/dt depends on Ω (more rapidly rotating star, more magnetic field, hotter the corona, larger the dm/dt)
  - R_A depends on Ω (although not in a straightforward manner: more rapidly rotating star, more magnetic field, but also larger the density and velocity of wind).
- In general $j = k\Omega^{\alpha}$, where α typically > 1, although there are signs that for very large Ω, the α value becomes very small (saturation).

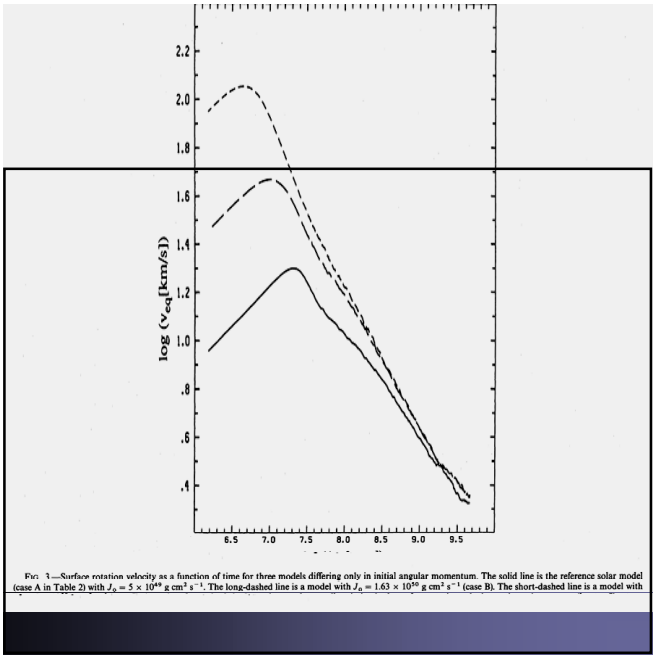

FIG. 3.—Surface rotation velocity as a function of time for three models differing only in initial angular momentum. The solid line is the reference solar model (case A in Table 2) with $J_0 = 5 \times 10^{48}$ g cm^2 s^{-1}. The long-dashed line is a model with $J_0 = 1.63 \times 10^{50}$ g cm^2 s^{-1} (case B). The short-dashed line is a model with

The solar atmosphere

The Sun's atmosphere

- The solar atmosphere is generally described as being composed of multiple layers, with the lowest layer being the photosphere, followed by the chromosphere, the transition region and the corona.
- In its simplest form it is modelled as a single component plane-parallel atmosphere.
- Density drops exponentially: $\rho(z) = \rho_0 \exp(-z/H_\rho)$ (for isothermal atmosphere). T=6000K ➔ $H_\rho \approx 100\text{km}$
- Mass of the solar atmosphere ≈ mass of the Indian ocean (≈ mass of the photosphere)
- Mass of the chromosphere ≈ mass of the Earth's atmosphere

1-D stratification

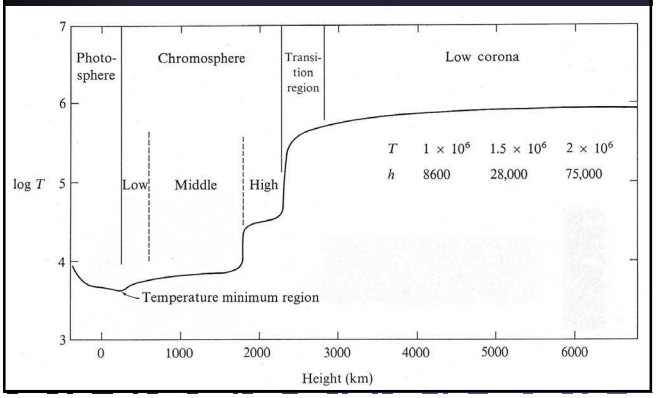

How good is the 1-D approximation?

- 1-D models reproduce extremely well large parts of the spectrum obtained with low spatial resolution (see spectral synthesis slide)
- However, any high resolution image of the Sun shows that its atmosphere has a complex structure (as seen at almost any wavelength)
- Therefore: 1-D models may well describe averaged quantities relatively well, although they probably do not describe any part of the real Sun at all.

The photosphere

- The photosphere extends between the solar surface and the temperature minimum, from which most of the solar radiation arises.
- The visible, UV (λ> 1600Å) and IR (< 100μm) radiation comes from the photosphere.
- 4000 K < T(photosphere) < 6000 K
- T decreases outwards ➔ $B_\nu(T)$ decreases outward ➔ absorption spectrum
- LTE is a good approximation
- Energy transport by convection and radiation
- Main structures: Granules, sunspots and faculae

The Sun in White Light

(limb darkening removed)

MDI on SOHO

Sunspots

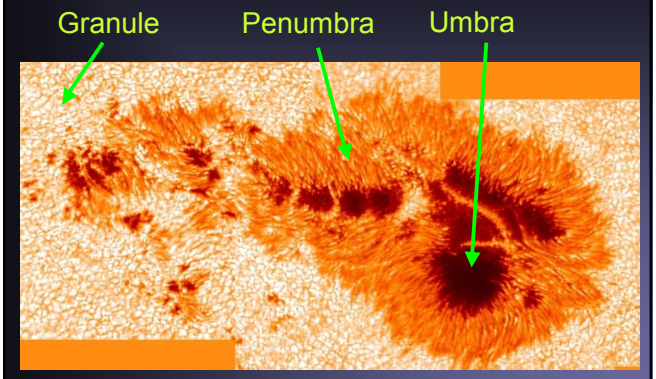

H. Schleicher, KIS/VTT, Obs. del Teide, Tenerife

Granulation

- Physics of convection and the properties of granulation and supergranulation have been discussed earlier, so that we can skip them here.

Chromosphere

- Layer lying just above the photosphere, at which the temperature appears to be increasing outwards (classically forming a temperature plateau at around 7000 K)
- Assumption of LTE breaks down
- Energy transport mainly by radiation and waves
- Assumption of plane parallel atmosphere is very likely to break down as well.
- Strong evidence for a spatially and temporally inhomogeneous chromosphere (gas at T<4000K is present beside gas with T>8000 K)

Chromospheric structure

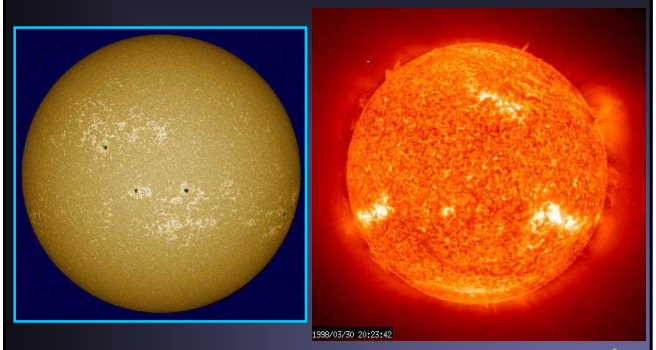

7000 K gas Ca II K

5 10^4 K gas (EIT He 304 Å)

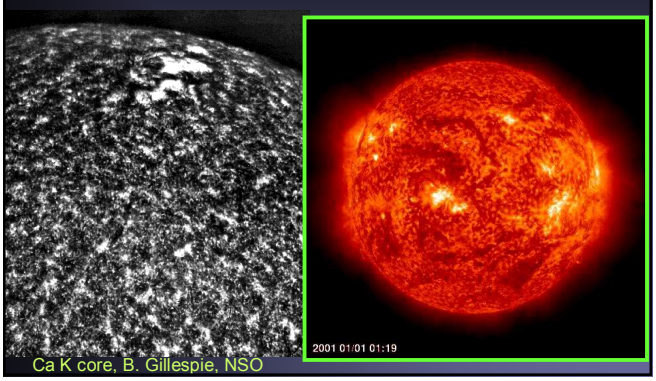

Ca K core, B. Gillespie, NSO

Chromospheric structure II

- The chromosphere exhibits a very wide variety of structures. E.g.,
  - Sunspots and Plages
  - Network and internetwork (grains)
  - Spicules
  - Prominences and filaments
  - Flares and eruptions

DOT Ca II K core Chromosphere DOT G-band photosphere

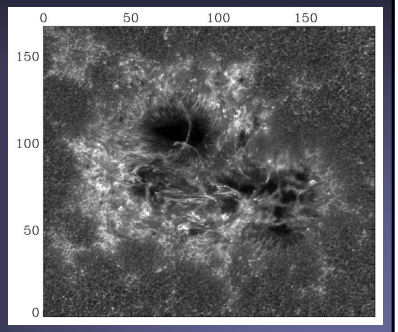

Chromospheric structure

- The chromosphere exhibits a very wide variety of structures. E.g.,
  - Sunspots and Plages
  - Network and internetwork
  - Spicules
  - Prominences and filaments
  - Flares and eruptions

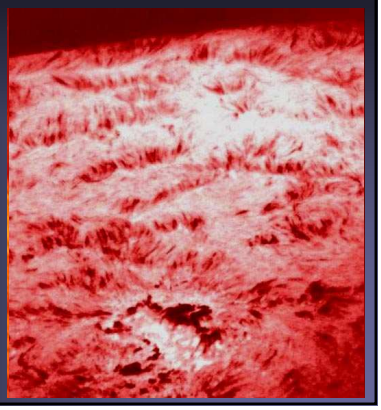

Chromospheric structure

- The chromosphere exhibits a very wide variety of structures. E.g.,
  - Sunspots and Plages
  - Network and internetwork
  - Spicules
  - Prominences and filaments
  - Flares and eruptions

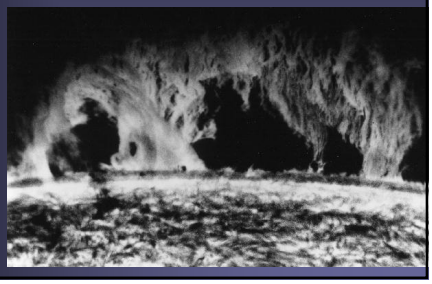

Chromospheric dynamics (DOT)

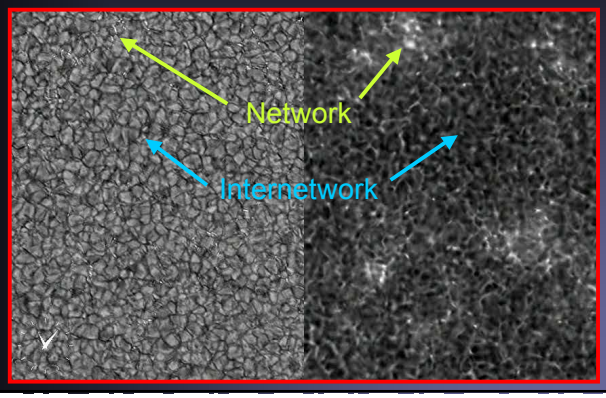

Chromospheric dynamics

- Oscillations, seen in cores of strong lines
- Power at 3 min in Inter-network
- Power at 5-7 min in Network

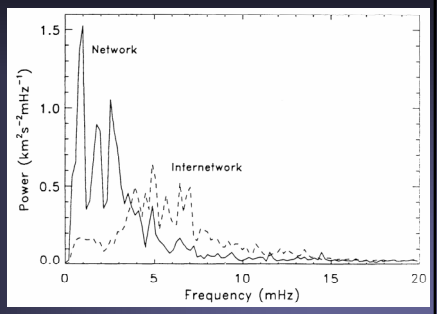

Lites et al. 2002

Models: the classical chromosphere

- Classical picture: plane parallel, multi-component atmospheres
- Chromosphere is composed of a gentle rise in temperature between T_{min} and transition region.

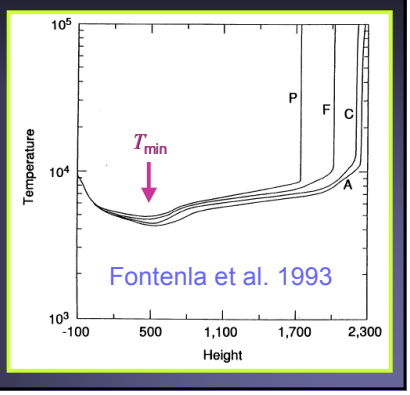

Fontenla et al. 1993

Need to heat the chromosphere

- Radiative equilibrium, RE: only form of energy transport is radiation & atmosphere is in thermal equilibrium.
- VAL-C: empirical model
- Dashed curves: temp. stratifications for increasing amount of heating (from bottom to top).

➔ Mechanical heating needed to reproduce obs.

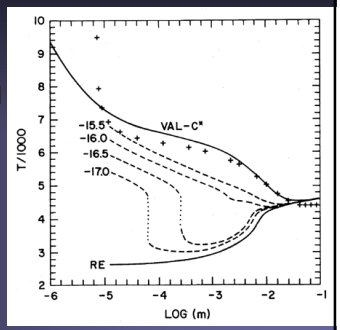

Anderson & Athay 1993

Dynamic models

- Start with piston in convection zone, consistent with obs. of photospheric oscillations
- Waves with periods of ≤3min propagate into chromosphere
- Energy conservation ($\rho v^2/2 = \text{const.}$) & strong ρ decrease ➔ wave amplitudes increase with height: waves steepen and shock
- Temp. at chromospheric heights varies between 3000 K and 10000 K

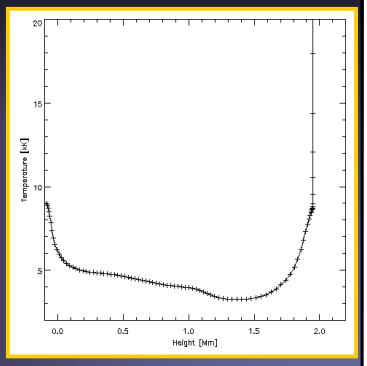

Carlsson & Stein

Transition Region

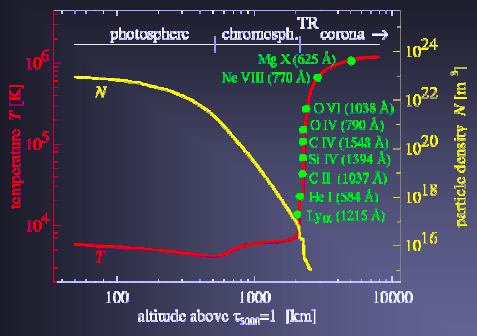

Semi-empirical 1D-models of solar atmosphere: steep increase of T in transition region (TR): < 100 km thick

TR spatial structure

- Lower transition region (T<5 10^5 K) shows structure very similar to chromosphere, with network, plage etc.
- C IV (10^5 K) imaged by SUMER
- In upper transition region structures are more similar to corona

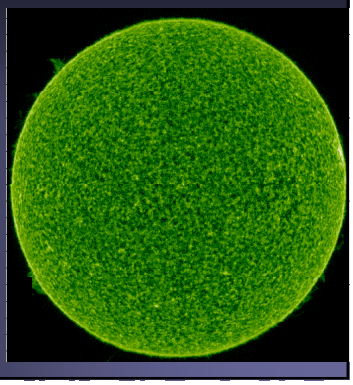

TR dynamic phenomena: blinkers

- Brightness variability in the (quiet) transition region is larger than in any other layer of solar atmosphere
- Typical brightening: blinkers
- Occur everywhere, all the time. Last for minutes to hours. How much of the brightening is due to overlapping blinkers?
- 1 time step ≈ 1 minute

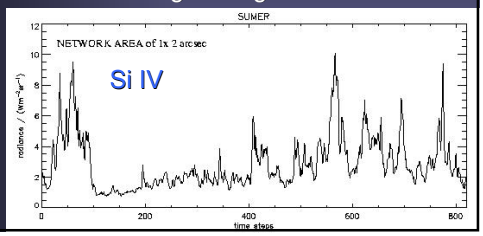

Explosive events

- Broadenings of TR spectral lines at 1-3 10^5 K
- Typical "normal" line width 20 km/s, in explosive event: up to 400 km/s. Cover only a few 1000 km and last only a few minutes
- Typically a few 1000 present on Sun at any given time

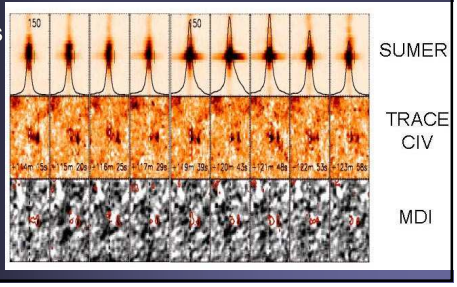

The Solar Corona

While the surface is about 6,000 K, the temperature in the corona reaches about 2 million K.

What causes this rapid increase in temperature is still one of the big mysteries in solar physics.

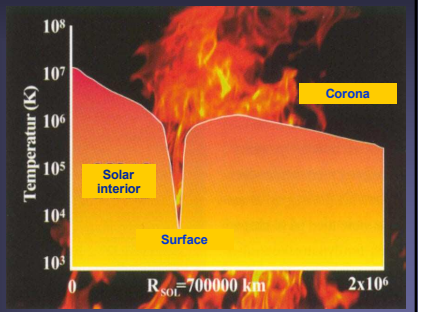

The Hot and Dynamic Corona

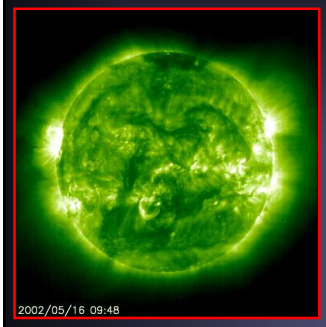

EUV Corona: 10^6 K plasma
(EIT/SOHO 195 Å)

White light corona
(LASCO C3 / SOHO, MPAe)

Solar corona during eclipses

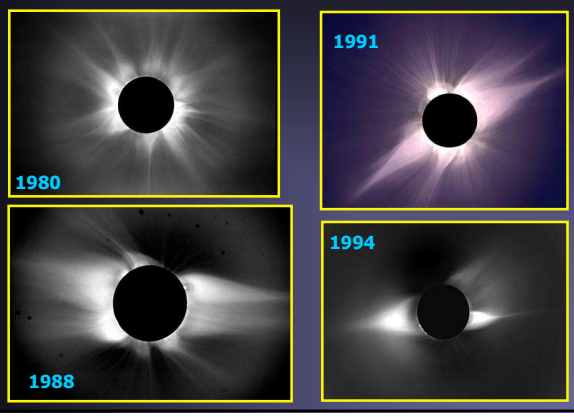

Coronal structures

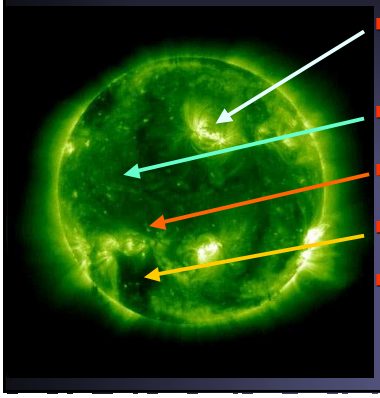

- Active regions (loops)
- Quiet Sun
- X-ray bright points
- Coronal holes
- Arcades

Fe XII 195 Å
(1.500.000 K)
17 May - 8 June 1998

Coronal structure: active region loops

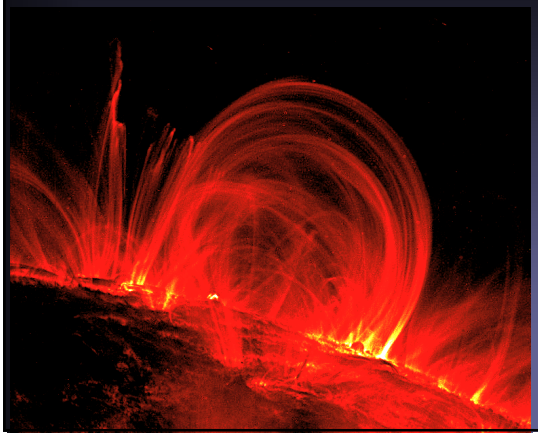

TRACE, 1999

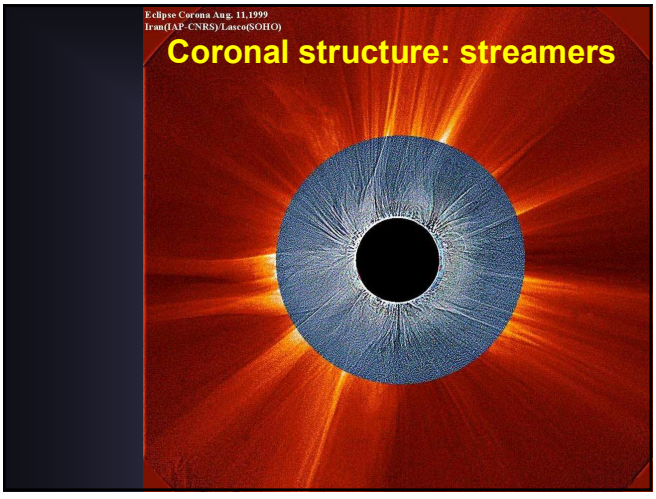

The solar wind

A constant stream of particles flowing from the Sun's corona, with a temperature of about a million degrees and with a velocity of about 450 km/s. The solar wind reaches out beyond Pluto's orbit, with the heliopause located roughly at 100-120 AU

Comets and the solar wind

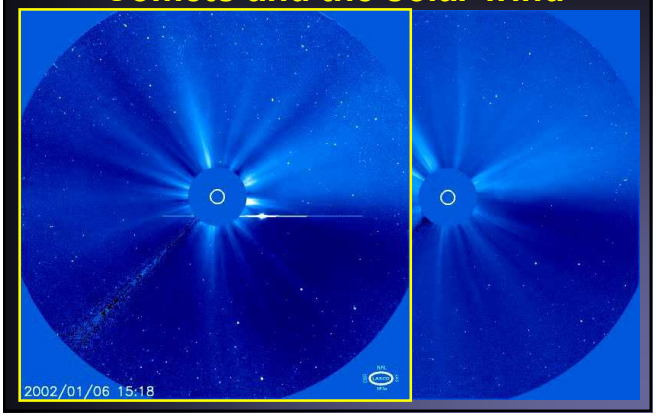

Solar wind characteristics at 1AU

Fast solar wind
- speed > 400 km/s
- $n_p \approx 3$ cm^{-3}
- homogeneous
- B≈ 5 nT = 0.0005G
- 95% H, 4% He
- Alfvenic fluctuations
- Origin: coronal holes coronal

Slow solar wind
- <400 km/s
- ≈ 8 cm^{-3}
- high variability
- B < 5 nT
- 94% H, 5% He
- Density fluctuations
- Origin: in connection with streamers

Transient solar wind
- speed from < 300 km/s up to >2000 km/s
- Variable B, with B up to 100 nT (0.01G)
- Often very low density
- Sometimes up to 30% He
- Often associated with interplanetary shock waves
- Origin: CMEs

3-D structure of the Solar Wind: Variation over the Solar Cycle

1st Orbit: 3/1992 - 11/1997
declining / minimum phase

2nd Orbit: 12/1997 - 2/2002
rising / maximum phase

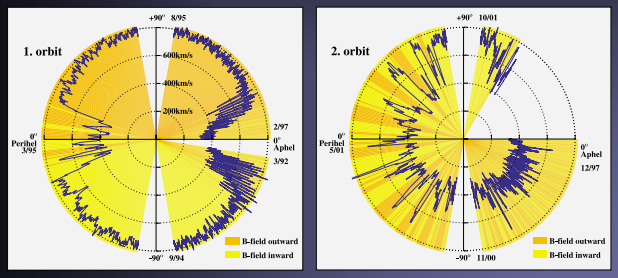

Ulysses SWICS data — Woch et al. GRL

Coronal Shape & Solar Wind: Ulysses Data & 3D-Heliosphere

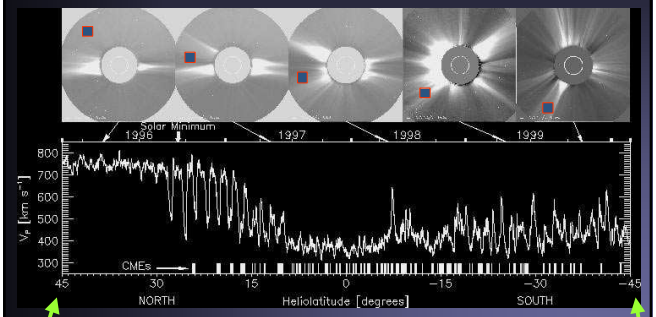

Activity minimum — Activity maximum

Parker's theory of the solar wind

- Basic idea: dynamic equilibrium between hot corona and interstellar medium. Mass and momentum balance equations:

$$\frac{d}{dr}(\rho r^2 v) = 0$$

$$v\frac{dv}{dr} = -\frac{1}{\rho}\frac{dP}{dr} - \frac{GM}{r^2}$$

➔ Parker's Eq. for solar wind speed (isothermal atmosphere)

$$\frac{1}{v}\frac{dv}{dr}(v^2 - c_S^{\,2}) = \frac{2c_S^{\,2}}{r} - \frac{GM}{r^2}$$

Parker's solar wind solutions

- Parker found 4 families of solar wind solutions
- 2 not supported by Obs. (supersonic at solar surface)
- 1 does not give sufficient pressure against the interstellar medium.
- Correct solution must be thick line in Fig.

CHECK WHY ONLY ONE SOLN IS CORRECT!!!!!!!!

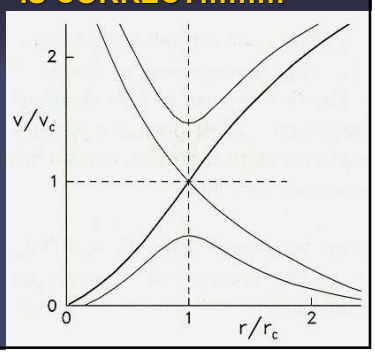

Solar wind speed

- Speed of solar wind predicted by Parker's model for different coronal temperatures (simple, isothermal case; no magnetic field)

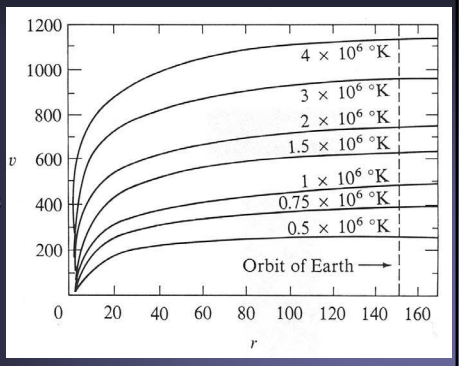

The Heliosphere

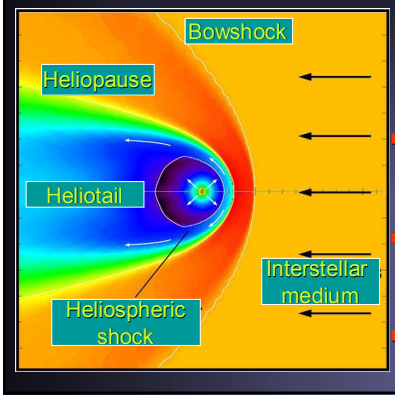

- Heliosphere = region of space in which the solar wind and solar magnetic field dominate over the instellar medium and the galactic magnetic field.
- Bowshock: where the interstellar medium is slowed relative to the Sun.
- Heliospheric shock: where the solar wind is decelerated relative to Sun
- Heliopause: boundary of the heliosphere

Magnetic Field

The source of the Sun's activity is the magnetic field

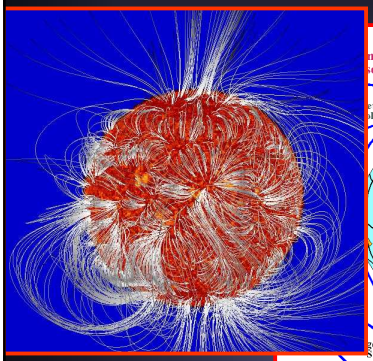

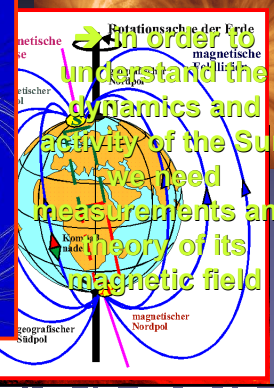

In order to understand the dynamics and activity of the Sun we need measurements and theory of its magnetic field

Thomas Wiegelmann

Correlation of field with brightness

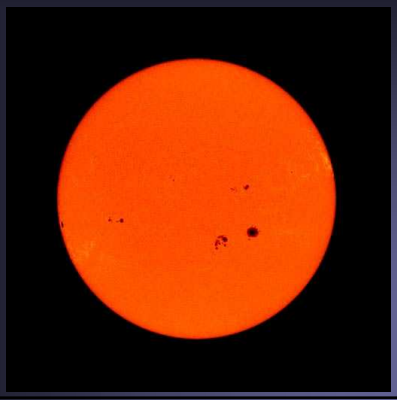

Open and closed magnetic flux

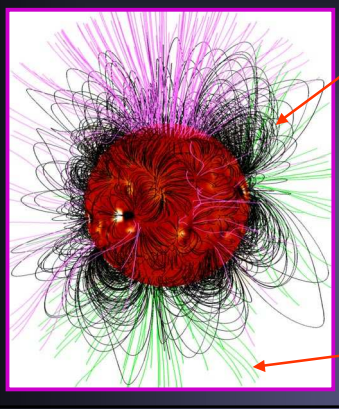

Closed flux: slow solar wind

Most of the solar flux returns to the solar surface within a few $R_\odot$ (closed flux)

A small part of the total flux through the solar surface connects as open flux to interplanetary space

Open flux: fast solar wind

Measured Magnetic Field at Sun's Surface

Month long sequence of magnetograms (approx. one solar rotation)

MDI/SOHO May 1998

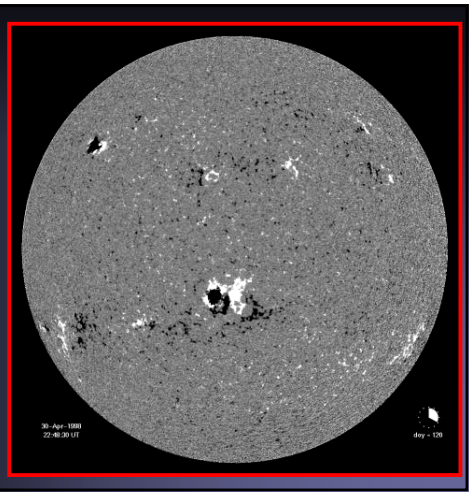

Methods of magnetic field measurement

- Direct methods:
  - Zeeman effect → polarized radiation
  - Hanle effect → polarized radiation
  - Gyroresonance → radio spectra
- Indirect methods: Proxies
  - Bright or dark features in photosphere (sunspots, G-band bright points)
  - Ca II H and K plage
  - Fibrils seen in chromospheric lines, e.g. Hα
  - Coronal loops seen in EUV or X-radiation

Example of proxies: Continuum vs. G-band

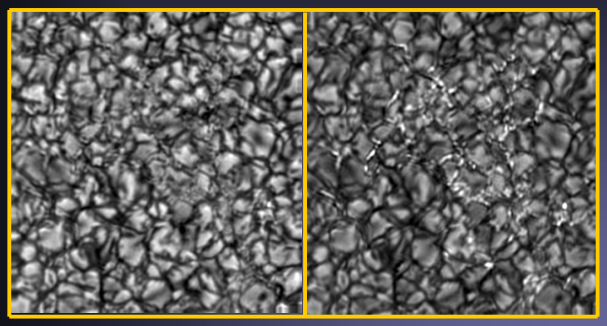

Continuum G-band

Ca II K as a magnetic field proxy

- Ca II H and K lines, the strongest lines in the visible solar spectrum, show a strongly increasing brightness with non-spot magnetic flux.
- The increase is slower than linear
- Magnetic regions (except sunspots) appear bright in Ca II: Ca plage and network regions

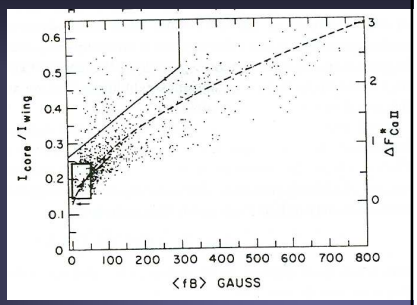

Hα and the chromospheric field

- Hα images of active regions show a structure similar to iron filing around a magnet. Do they (roughly) follow the field lines?
- Relatively horizontal field in chromosphere?
- Note spiral structure around sunspot.

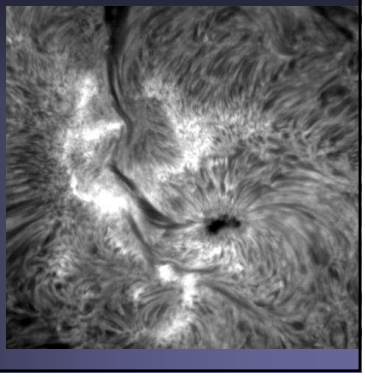

Zeeman diagnostics

- Direct detection of magnetic field by observation of magnetically induced splitting and polarisation of spectral lines
- Important: Zeeman effect changes not just the spectral shape of a spectral line (often subtle and difficult to measure), but also introduces a unique polarisation signature

→ Measurement of polarization is central to measuring solar magnetic fields.

Polarized radiation

- Polarized radiation is described by the 4 Stokes parameters: I, Q, U and V

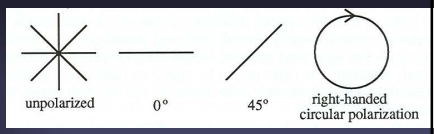

- I = total intensity = $I_{lin}(0^o) + I_{lin}(90^o) = I_{lin}(45^o) + I_{lin}(135^o) = I_{circ}(right) + I_{circ}(\text{left})$
- $Q = I_{lin}(0^o) - I_{lin}(90^o)$
- $U = I_{lin}(45^o) - I_{lin}(135^o)$
- $V = I_{circ}(\text{right}) - I_{circ}(\text{left})$
- Note: Stokes parameters are sums and differences of intensities, i.e. they are directly measurable

Zeeman splitting of atomic levels

- In the presence of a B-field a level with total angular moment J will split into $2J+1$ sublevels with different M.
- $E_{J,M} = E_J + \mu_0 g M_J B$
- Transitions are allowed between levels with $\Delta J = 0, \pm 1$ & $\Delta M = 0$ (π), ± 1 (σ_b, σ_r)
- Splitting is determined by Lande factor g :
  $g(J,L,S) = 1+(J(J+1)+S(S+1)-L(L+1))/2J(J+1)$

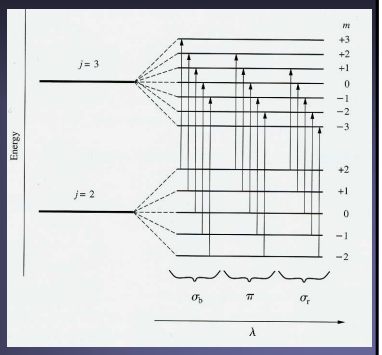

Splitting patterns of lines

- Depending on g of the upper and lower levels, the spectral line shows different splitting patterns
- Positive: π components: $\Delta M = 0$
- Negative: σ components: $\Delta M = \pm 1$
- Top left: normal Zeeman effect (rare)
- Rest: anomalous Zeeman effect (usual)

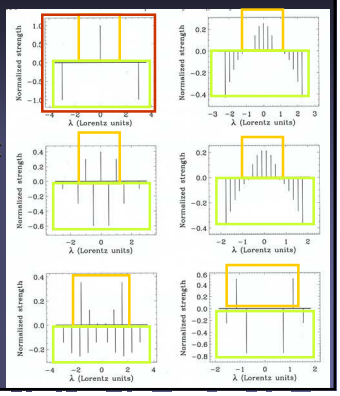

Polarization and Zeeman effect

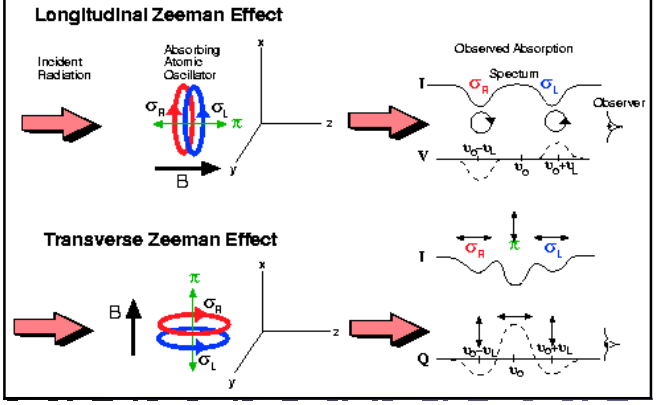

Effect of changing field strength

Formula for Zeeman splitting (for B in G, λ in Å):

$\Delta\lambda_H = 4.67\ 10^{-13}\ g_{eff} B \lambda^2$ [Å]

g_{eff}=effective Lande factor of line

For large B: $\Delta\lambda_H$ = Δλ between σ-component peaks

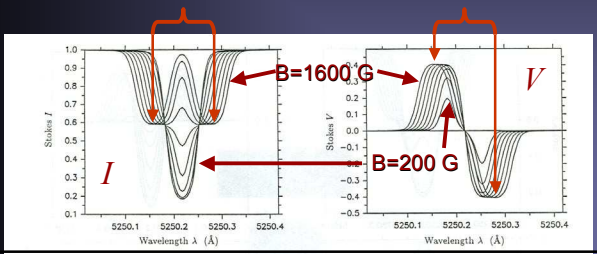

Dependence on B, γ, & φ

- $I \sim \kappa_\sigma(1+\cos^2\gamma)/4 + \kappa_\pi \sin^2\gamma/2$
- $Q \sim B^2 \sin^2\gamma \cos 2\varphi$
- $U \sim B^2 \sin^2\gamma \sin 2\varphi$
- $V \sim B \cos\gamma$

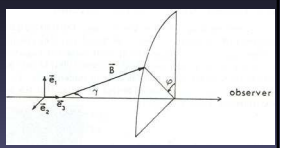

- Q, U: transverse component of B
- V: longitudinal component of B

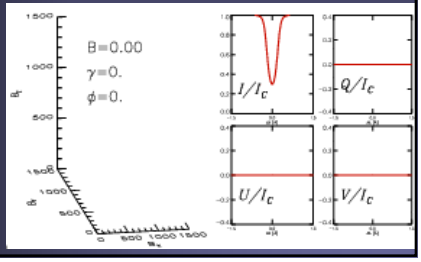

Juanma Borrero

Zeeman polarimetry

- Most used remote sensing of astrophysical (and certainly solar) magnetic fields
- Effective measurement of field strength if Zeeman splitting is comparable to Doppler width or more: $B > 200$ G … 1000 G (depending on spectral line) ➔ works best in photosphere
- Splitting scales with λ ➔ works best in IR
- Sensitive to cancellation of opposite magnetic polarities ➔ needs high spatial resolution

Effect of wavelength of spectral line

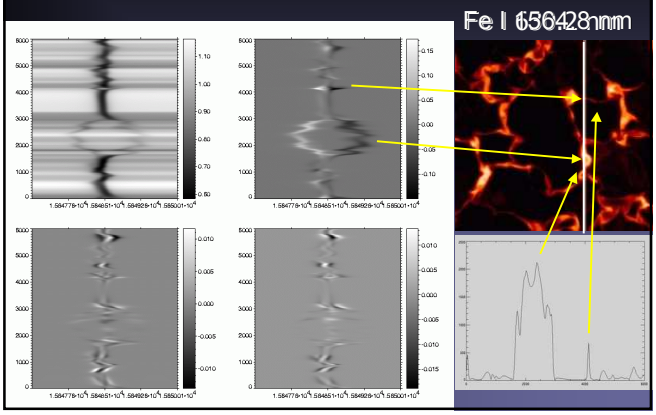

Cancellation of magnetic polarity

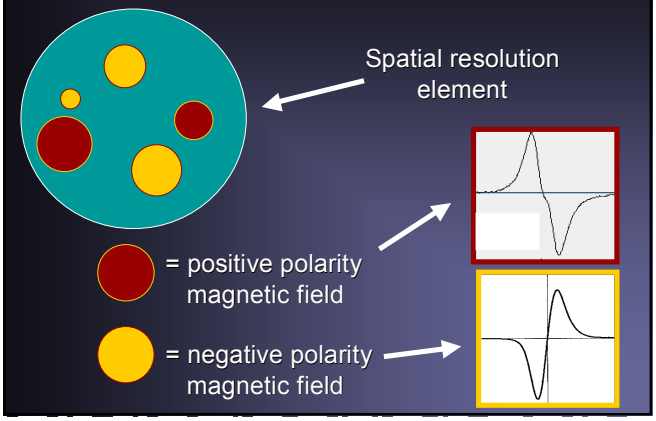

Magnetograms

- Magnetograph: Instrument that makes maps of (net circular) polarization in wing of Zeeman sensitive line.
- Example of magnetogram obtained by MDI
- Conversion of polarization into magnetic field requires a careful calibration.

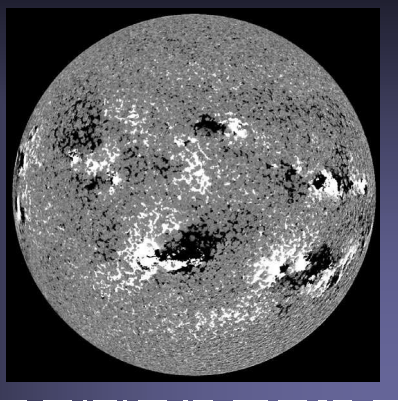

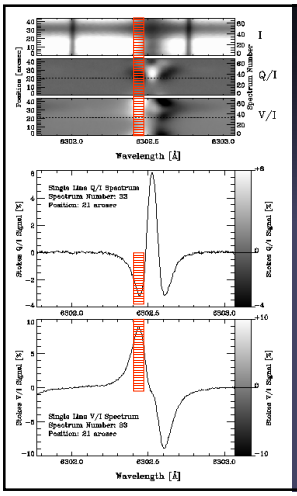

What does a magnetogram show?

- Plotted at left:
  - Top: Stokes I, Q and V along a spectrograph slit
  - Middle: Sample Stokes Q profile
  - Bottom: Sample Stokes V profile
  - Red bars: example of a spectral range used to make a magnetogram. Generally only Stokes V is used (simplest to measure), gives longitudinal component of B.

Synoptic charts

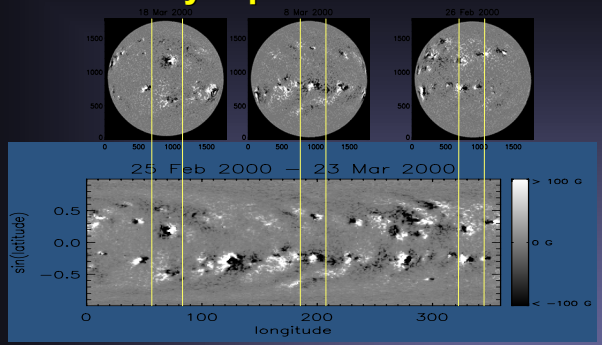

Synoptic maps approximate the radial magnetic flux observed near the central meridian over a period of 27.27 days (= 1 Carrington rotation)

Polarized radiative transfer

- Complication: RTE required for 4 Stokes parameters: Written as differential equation for Stokes vector $\mathbf{I}_\nu = (I_\nu, Q_\nu, U_\nu, V_\nu)$
- Eq. in plane parallel atmosphere for a spectral line (Unno-Rachkowsky equations):

  $\mu \, d\mathbf{I}_\nu / d\tau_c = \mathbf{\Omega}_\nu \mathbf{I}_\nu - \mathbf{S}_\nu$
- $\mathbf{\Omega}_\nu$ = absorption matrix (basically ratio of line to continuum absorption coefficient), $\mathbf{S}_\nu$ = source function vector, τ_c = continuum optical depth.

Polarized radiative transfer II

The absorption matrix

$$\mathbf{\Omega}_\nu = \begin{pmatrix} 1+\eta_I & \eta_Q & \eta_U & \eta_V \\ \eta_Q & 1+\eta_I & -\rho_V & \rho_U \\ \eta_U & \rho_V & 1+\eta_I & \rho_Q \\ \eta_V & -\rho_U & -\rho_Q & 1+\eta_I \end{pmatrix}$$

SAY MORE ABOUT MATRIX ELEMENTS!!!!!! SHOW HOW ZEEMAN EFFECT ENTERS INTO THEM, ETC.!!!!!

Polarized radiative transfer III

- The Zeeman effect only enters through $\mathbf{\Omega}_\nu$
- $\mathbf{\Omega}_\nu$ contains besides absorption due to Zeeman-split line (η_I, η_Q, η_U, η_V) also magnetooptical effects, such as Faraday rotation (ρ_Q, ρ_U, ρ_V) : rotation of plane of polarization when light passes through B.
- $\mathbf{\Omega}_\nu = \mathbf{\Omega}_\nu(\gamma, \varphi, B)$, i.e. $\mathbf{\Omega}_\nu$ depends on the full magnetic vector (in addition to the usual quantities that the absorption coefficient depends on)

LTE

- In LTE the Unno-Rachkowsky equations simplify since

  $\mathbf{S}_\nu = (B_\nu, 0, 0, 0)$

  Here B_ν = Planck function
- Also, $\mathbf{\Omega}_\nu$ is simplified. The η_I, η_Q, η_U, η_V and ρ_Q, ρ_U, ρ_V values only require application of Saha-Boltzmann equations (similar situation as for LTE in case of normal radiative transfer). Each of these quantities is, of course, frequency dependent.

Solution of Unno Eqs

- General solution best done numerically (even formal solution is non-trivial: exponent of matrix $\mathbf{\Omega}_\nu$)
- Simple analytical solutions exist for a Milne-Eddington atmosphere (i.e. for $\mathbf{\Omega}_\nu$ independent of τ_ν and $\mathbf{S}_\nu$ depending only linearly on τ_ν). Particularly simple if we neglect magneto-optical effects
- $I(\mu) = \beta \, \mu \, (1+\eta_I)/\Delta$
- $P(\mu) = \beta \, \mu \, \eta_P/\Delta$, where $P = Q, U,$ or V
- $\Delta = (1+\eta_I)^2 - \eta_Q^2 - \eta_U^2 - \eta_V^2$

  takes care of line saturation
- β is derivative of Planck function with respect to τ_ν .

Basics: magnetic pressure

- Magnetic field exerts a pressure. Pressure balance between two components of the atmosphere, 1 and 2 (Gauss units):

$$\frac{B_1^2}{8\pi} + P_1 = P_2 + \frac{B_2^2}{8\pi}$$

- If, e.g. $B_2 = 0$, then $P_1 < P_2$ and it follows:

➔ Magnetic features are evacuated compared to surroundings.

- If $B_2 = 0$ and $T_1 = T_2$, then also $\rho_1 < \rho_2$, so that the magnetic features are buoyant compared to the surrounding gas.
- In the convection zone this buoyancy means that rising field bundles (flux tubes) keep rising (unless stopped by other forces, e.g. curvature forces.

Basics: plasma β

- Plasma β describes the ratio of thermal to magnetic energy density:

$$\beta = \frac{8\pi P}{B^2}$$

- $\beta < 1$ ➔ Magnetic field dominates and dictates the dynamics of the gas
- $\beta > 1$ ➔ Thermal energy, i.e. gas dominates & forces the field to follow
- β changes with $r/R_\odot$
  - $\beta > 1$ in convection zone
  - $\beta < 1$ in atmosphere, particularly in corona $\beta << 1$

Supergranules and magnetic field

- Magnetogram: black and white patches
- Horizontal velocity: arrows
- Divergence: blue arrows > 0; red arrows: < 0
- Supergranule boundaries: yellow
- Magnetic field is concentrated at edges of supergranules

➔ B swept out by flow

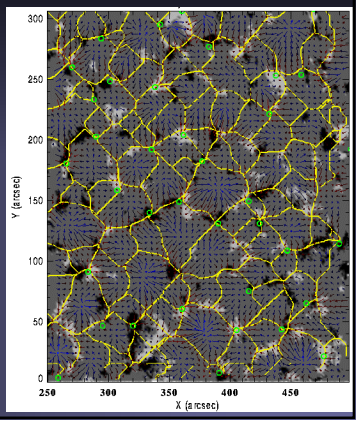

Frozen-in magnetic fields

- Magnetic field is swept to supergranule boundaries ➔ magnetic field is "frozen" into the plasma
- This happens if there are a sufficient number of ionised particles, or equivalently, if the electric conductivity is very high, since charged particles cannot cross field lines (gyration)
- This is the case, even in the cool photosphere of sunspots (only 10^{-4} of all particles are ionized), due to the large number of collisions

➔ If plasma moves perpendicularly to the field, it drags the field with it (or is stopped by the field) and vice versa. Flows parallel to the field are unaffected.

Magnetic field in the convection zone

- Magnetic field thought to be produced by a dynamo located near the bottom of the convection zone (e.g. in the overshoot layer below the convection zone).

➔ toroidal flux tubes

- Once field becomes strong enough, it is susceptible to buoyancy (Parker instability)
- A loop-like structure moves towards the solar surface and breaks out.

Emergence of a magnetic flux tube

Magnetic field is believed to be generated mainly in the Tachocline near bottom of convection zone.
Due to its buoyancy (see earlier slide; Parker instability), a magnetic field will rise towards the solar surface. At the solar surface it will produce a bipolar active region.

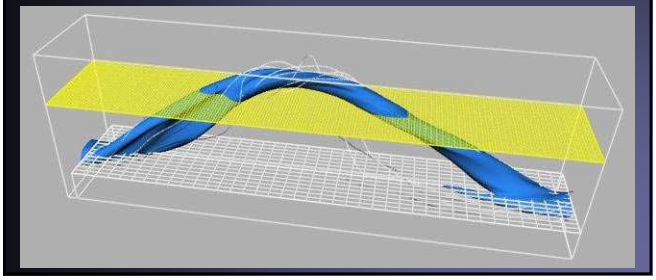

Emergence and evolution of active region: GET BETTER MOVIE!!!!!!!!!!

The photospheric field

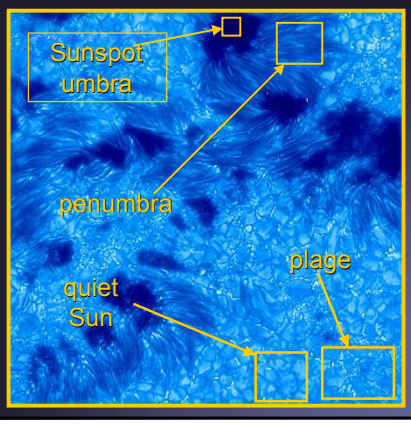

Sunspots

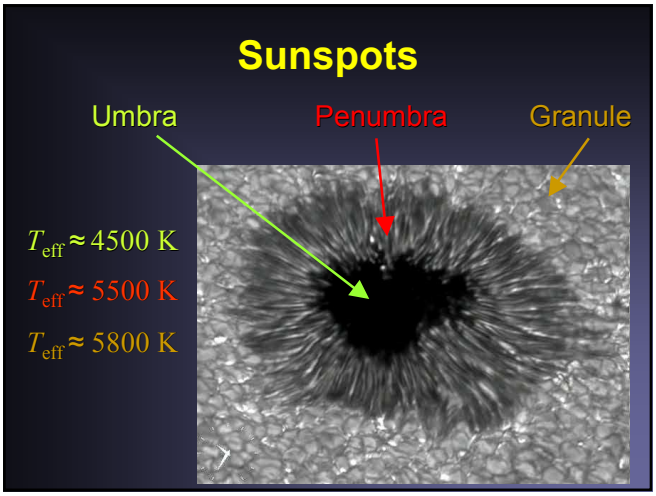

Sunspots, some properties

- Field strength: Peak values 2000-3500 G
- Brightness: umbra: 20% of quiet Sun, penumbra: 75%
- Sizes: Log-normal size distribution. Overlap with pores (log-normal = Gaussian on a logarithmic scale)
- Lifetimes: T between hours & months: Gnevyshev-Waldmeier rule: $A_{\rm max} \sim T$, where $A_{\rm max}$ = max spot area.

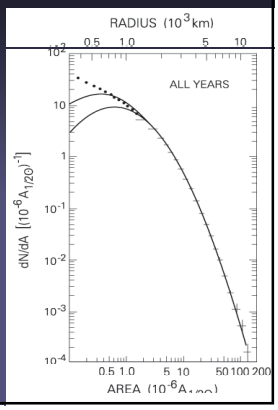

Why are sunspots dark?

- Basically the strong nearlly vertical magnetic field, not allowing motions across the field lines, quenches convection inside the spot.
- Since convection is the main source of energy transport just below the surface, less energy reaches the surface through the spot ➔ dark

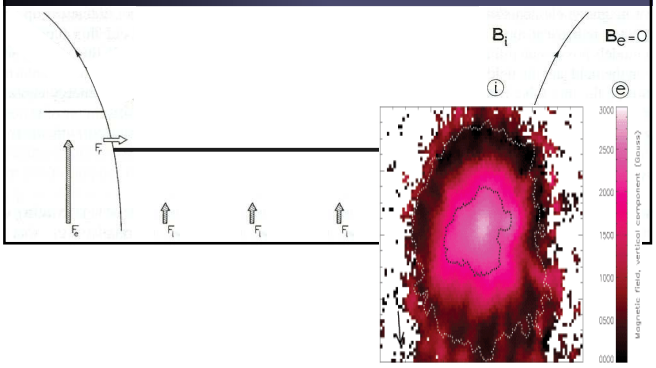

Why are sunspots dark? II

- Where does the energy blocked by sunspots go?
- Spruit (1982) showed: both heat capacity and thermal conductivity of CZ gas is very large

➔High thermal conductivity: blocked heat is redistributed throughout CZ (no bright rings around sunspots)

High heat capacity: the additional heat does not lead to a measurable increase in temperature

- In addition: time scale for thermal relaxation of the CZ is long, 10^5 years: excess energy is released almost imperceptibly.

Magnetic structure of sunspots

- Peak field strength ≈ 2000 – 3500 G (usually in darkest, central part of umbra)
- B drops steadily towards boundary, $B(R_{\rm spot}) \approx 1000$ G
- At centre, field is vertical, becoming almost horizontal near $R_{\rm spot}$.
- Regular spots have a field structure similar to a buried dipole

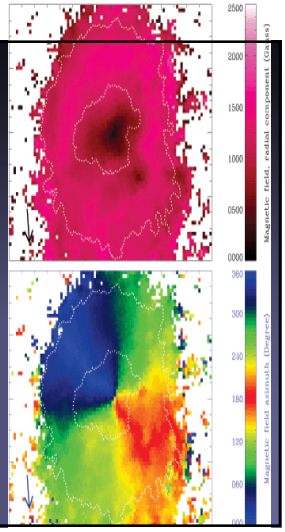

Magnetic structure of sunspots II

Azimuthal averages of the various magnetic field components in a sample of regular (near-circular) medium-sized sunspots.

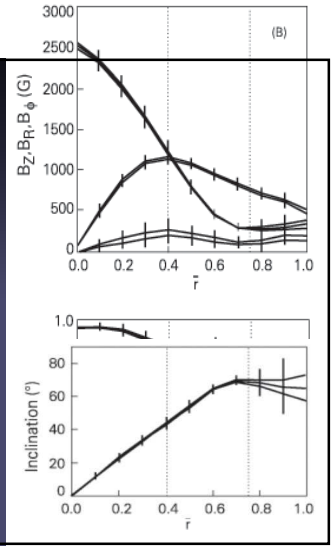

Magnetic structure of sunspots

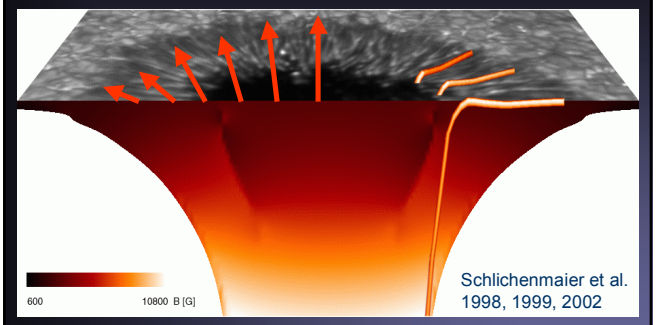

- Regular on large scales (≈ dipole, B_{max} ≈ 2500 G, for simple spots)
- Extremely complex on small scales (penumbra, subsurface)

Sunspot fine structure

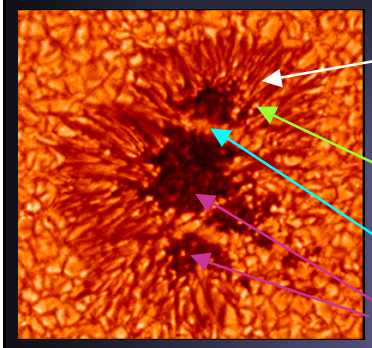

Highest resolution

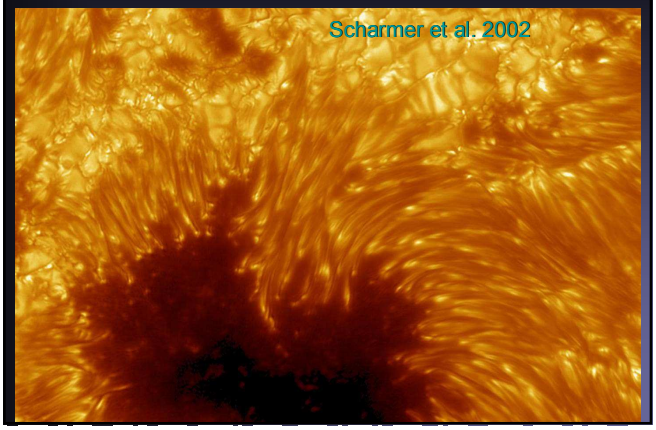

Sunspots

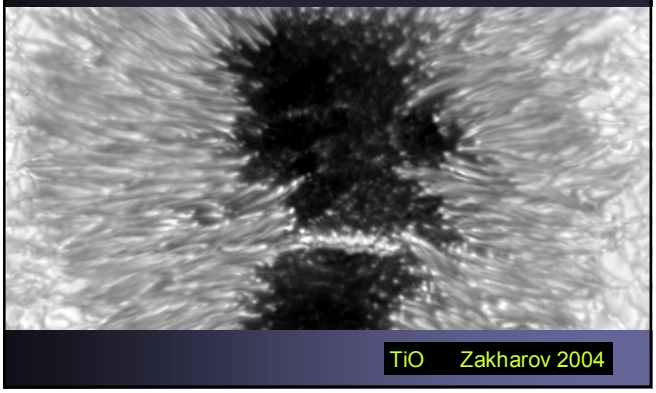

Umbral dots seen in TiO

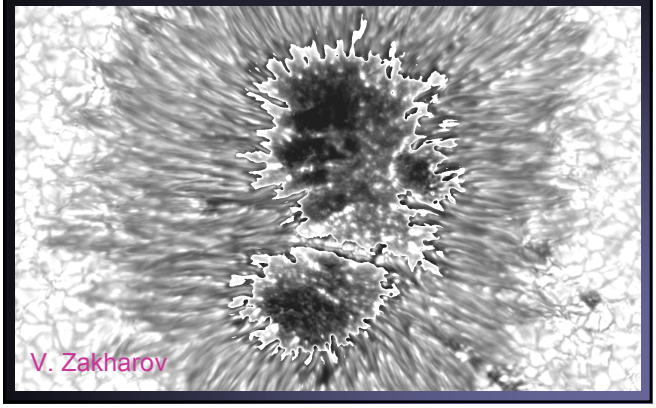

Magnetic structure of sunspots

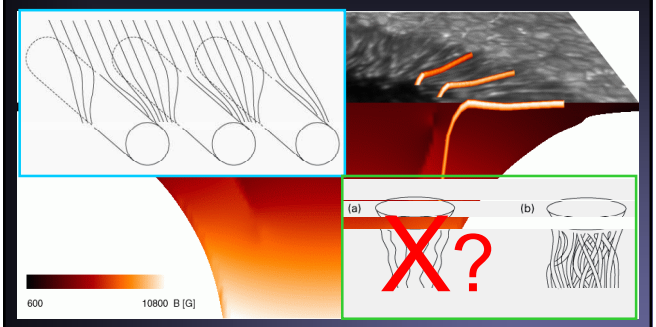

Sunspots span too many spatial and temporal scales to be successfully simulated from first principles.

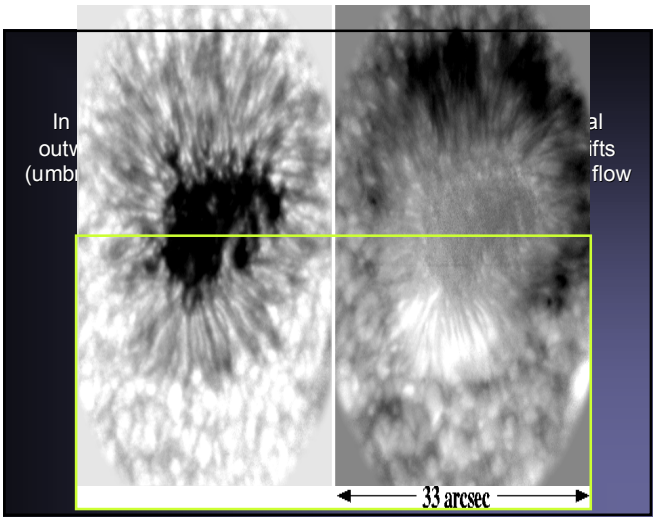

Evershed effect: illustration

- Horizontal outflow of matter.
- Thought to be driven by a siphon flow mechanism
- NEED NEW SLIDE !!!!!!!

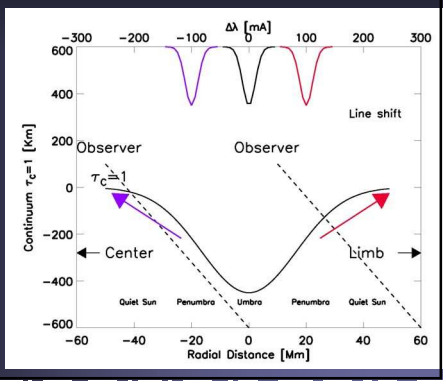

Siphon flow model of Evershed effect

- Proposed by Meyer & Schmidt (1968).
- If there is an imbalance in the field strength of the two footpoints of a loop, then gas will flow from the footpoint with lower B to that with higher B.
- Supersonic flows are possible.

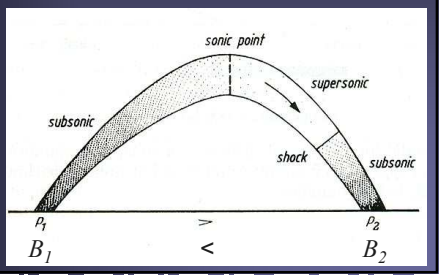

The Wilson effect

- Near the solar limb the umbra and centre-side penumbra disappear
- ➔We see 400-800 km deeper into sunspots than in photosphere
- Correct interpretation by Wilson (18th century).

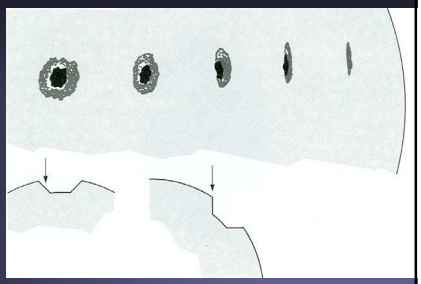

Other interpretation by e.g. W. Herschell: photosphere is a layer of hot clouds through which we see deeper, cool layers: the true, populated surface of the Sun.

Sunspot Wilson depression

Map of Wilson depression (determined from T & B measurements and assumption that sunspot magnetic field is close to potential)

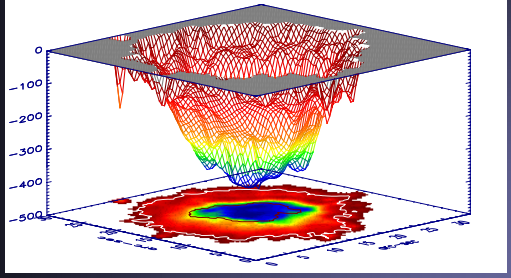

Shibu Mathew

What causes the Wilson depression?

- B square/8 pi means gas pressure lower in spot than outside i.e. density also lower, i.e. fewer atoms to absorb, i.e. opacity also lower
- we see deeper into spot

Magnetic elements

- Most of the magnetic flux on the solar surface occurs outside sunspots and pores (=smaller dark magnetic structures).
- These most common magnetic features, called magnetic elements, are small (diameters partly below spatial resolution of 100 km), bright and concentrated in network and facular regions.
- Magnetic elements are usually described by thin magnetic flux tubes (i.e. bundles of nearly parallel field lines).

Surprisingly constant field strength

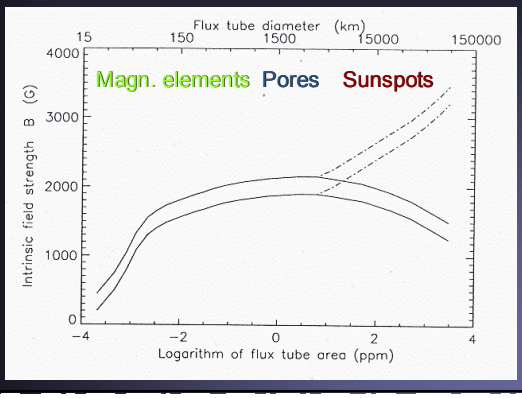

Temperature contrast vs. size

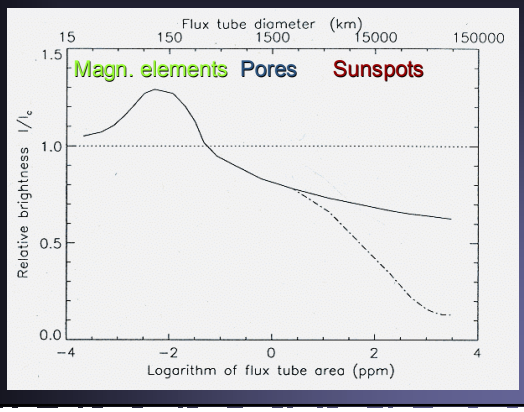

Temperature stratifications of quiet Sun, sunspot, plage

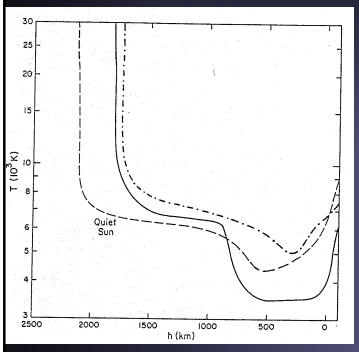

- Dashed line: Quiet Sun atmosphere
- Solid line: sunspot atmosphere
- Dot-dashed line: active region plage atmosphere
- Plage is hottest everywhere in atmosphere
- Sunspot coldest in photosphere, but gets hotter in chromosphere

Increased contrast of magnetic elements in higher layers

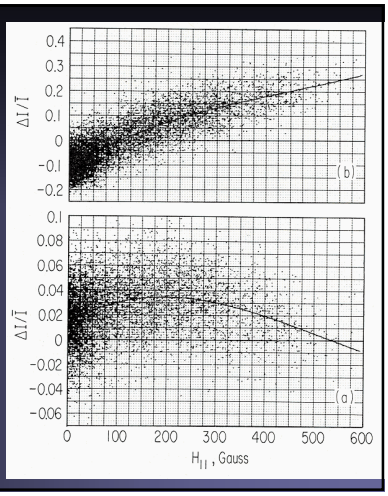

Why are magnetic elements bright?

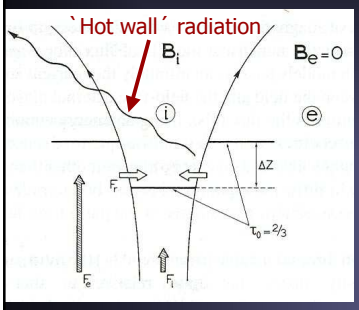

- Quenching of convection
- Partial evacuation
  - → enhanced transparency
  - → heating by `hot walls´
  - → *local flux excess*
- Inflow of radiation wins because the flux tubes are narrow (diameter ~ Wilson depression).
- High heat conductivity
  - → flux disturbance partly propagates into the deep convection zone
  - → Kelvin-Helmholtz time

Why are faculae best seen near limb?

The Sun in White Light, with limb darkening removed

MDI on SOHO

Flux tube brightening near limb

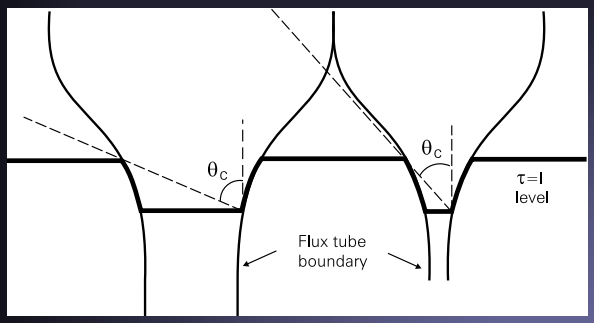

- The flux tubes expand with height (pressure balance
- They appear brightest when hot walls are well seen, i.e. near limb (closer to limb for larger tubes

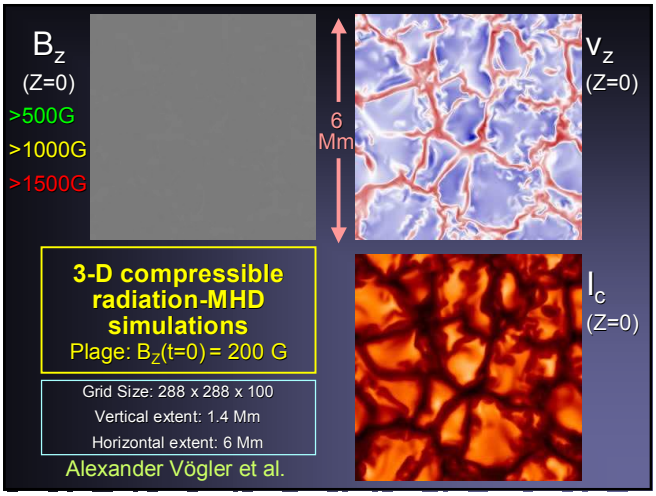

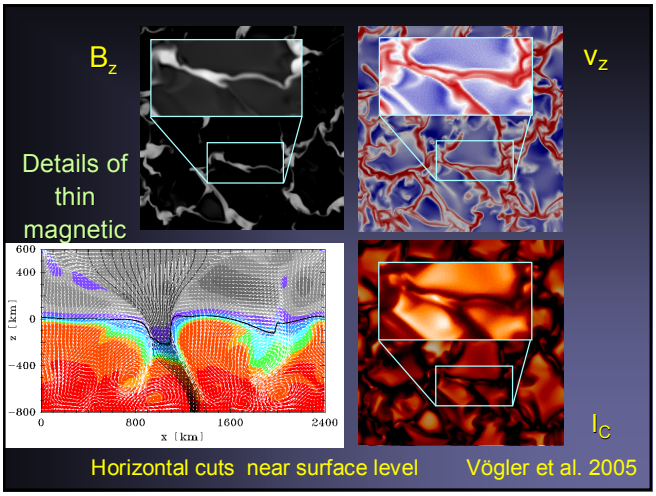

3-D Radiation-MHD Simulations

Alexander Vögler, Robert Cameron, Manfred Schüssler

Mixed polarity simulations: diffusion & cancellation of opposite polarities (20 km resolution): $\langle B_{initial} \rangle = 200$G.

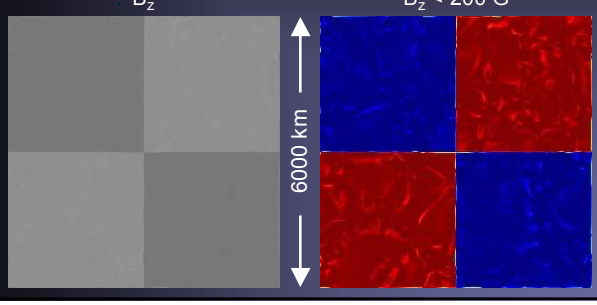

Simulations require computers...

G-band Spectrum Synthesis

G-Band (Fraunhofer): spectral range: 4295-4315 Å
contains many temperature-sensitive molecular lines (CH)

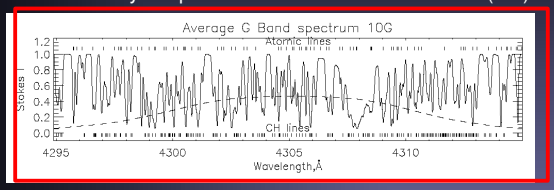

For comparison with observations, we define as G-band intensity the integral of the spectrum obtained from the simulation data:

$$I_G = \int_{4295\ A}^{4315\ A} I(\lambda) d\lambda$$

Shelyag et al. 2004

G-band: Simulation vs. Observation

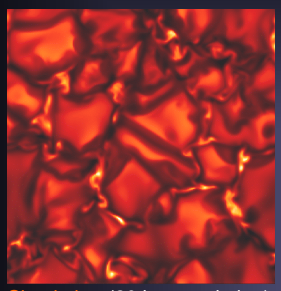

Simulation (20 km resolution)
Schüssler et al. 2003
Shelyag et al. 2004

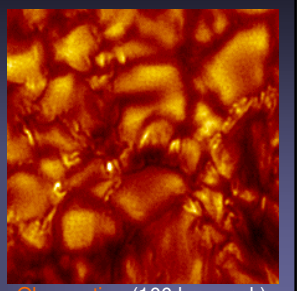

Observation (100 km resol.)
(SST, La Palma)
Scharmer et al. 2002

Stokes V asymmetry

- Stokes V profiles observed in quiet Sun and in active region plage are asymmetric: typically blue wing has larger area 'A' and amplitude 'a' than red wing

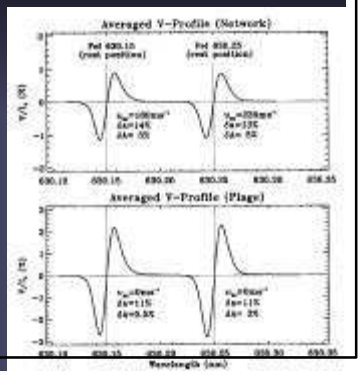

Producing Stokes V asymmetry

- Consider 2-layered atmosphere:
  - Bottom layer a: v but no B
  - Top layer b: B but no v
- Note the importance of line saturation for producing asymmetric V profile.

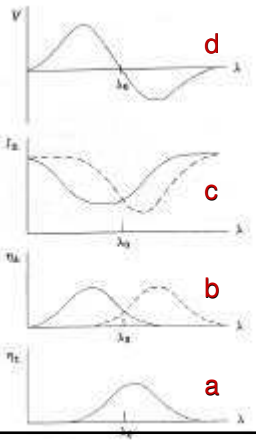

Flux Tubes, Canopies, Loops and Funnels

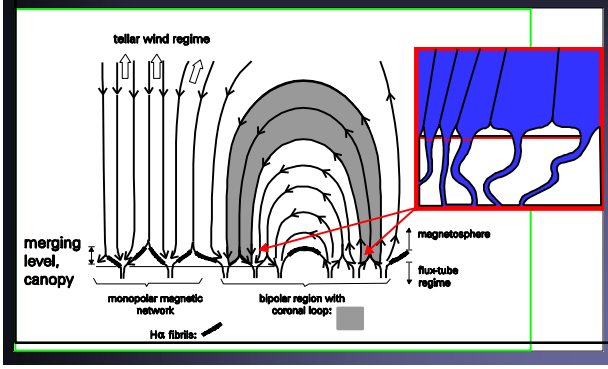

Measurement of *B* at coronal base

- Previously: Magnetic vector only known at solar surface. However, magnetic field has main effect in corona. Exception: radio observations give |B| but low resolution.
- Now: Direct measurement of full magnetic vector at base of corona & in cool loops possible
- Measurement using He I 10830 Å (TIP, VTT, Tenerife) & simple inversion code

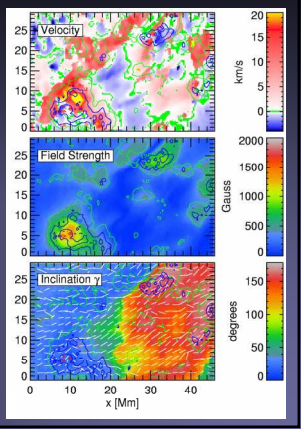

Solanki et al. 2003, Lagg et al. 2004

Structure of Magnetic Loops

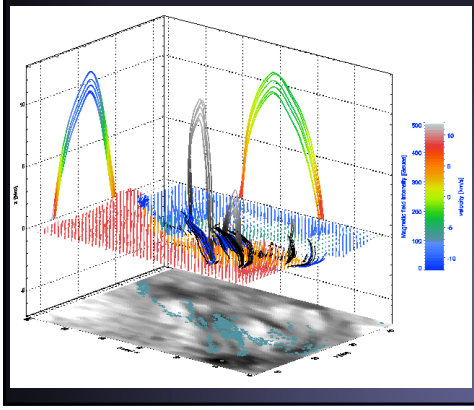

Magnetic loops deduced from measurements of He I 10830 Å

Stokes profiles in an emerging flux region.

Left projection: Field strength

Right projection: Vertical velocity

Andreas Lagg

Magnetic field extrapolations: Force free and potential fields

- General problem in solar physics: Magnetic field is measured mainly in the photosphere, but it makes the music mainly in the corona.

➔Either improve coronal field measurements or extrapolate from photospheric measurements into the corona.

- If $\beta << 1$ then we can neglect the influence of the gas on the field: the field is force-free. Considerable simplification of the computations
- If we further assume that there are no currents, the computations become even simpler (potential field).

Testing Magnetic Extrapolations

- Non-linear force-free fields reproduce the loops reconstructed from observations better than the linear force-free ones and far better than potential field extrapolations.
- Loops harbour strong currents while still emerging.

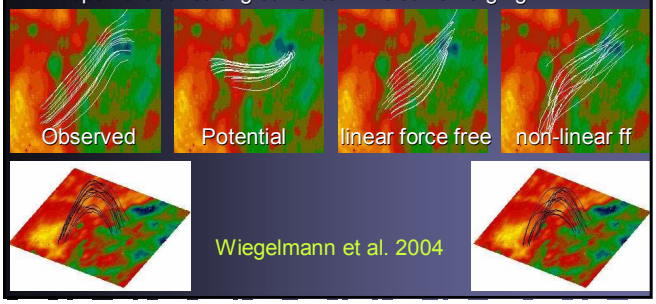

Wiegelmann et al. 2004

Prominences

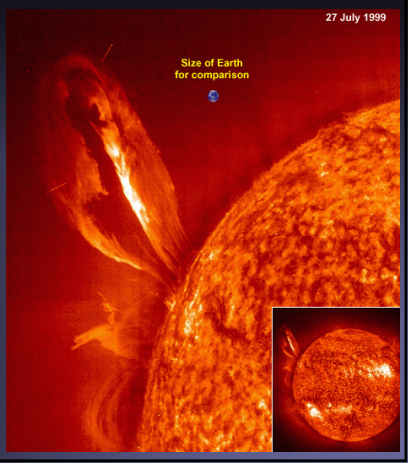

Kippenhahn's magnetic circus

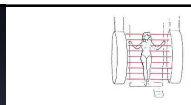

Problem: prominence material is dense and cool and high in the sky ➔ It must be supported against gravity. Obvious supporting structure: magnetic field. However, magnetic field must be curved upwards to keep the material from flowing down along the field lines. Different solutions have been proposed.

Prominence models

Kippenhahn-Schlüter (below), Kuperus-Raadu (below right) and flux tube (right)

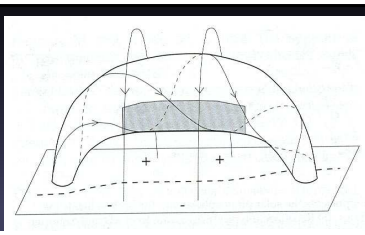

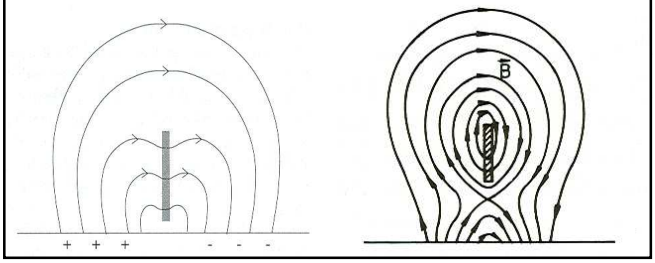

Large scale magnetic structure of the quiet Sun

- At large scales dipolar component of the magnetic field survives, since multipoles ➔ $B \sim r^{-n-1}$, where n=2 for dipole, n=3 for quadrupole, etc.
- Closer to sun ever higher order multipoles are important

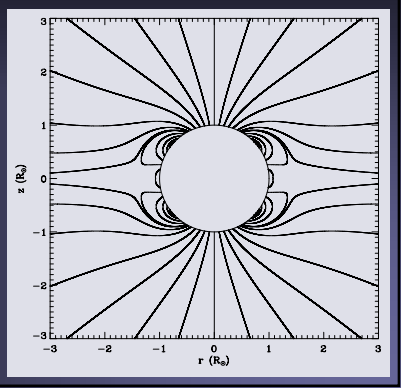

Solar current sheet at activity minimum

- At activity minimum solar magnetic field is like a dipole, whose field lines are stretched out by the solar wind.
- Field lines with opposite polarity lie close to each other near equator: euatorial current sheet.
- If dipole axis inclined to ecliptic: magnetic polarity at Earth changes over solar rotation.

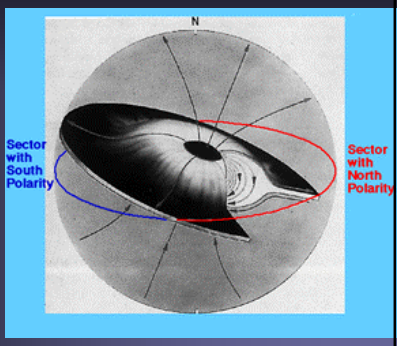

Heliospheric current sheet and Parker spiral

- Since solar wind expands radially beyond the Alfven radius (where the energy density in the wind exceeds that in the magnetic field) and the Sun rotates (i.e. the footpoints of the field), the structure of the field (carried out by the wind, but anchored on rotating surface) shows a spiral structure.